Geochemical Numerical Simulation of Low Salinity Waterflooding in Sandstone Reservoirs

Oubai Mishal Abdelrasool Elagab (oubaielagab@gmail.com)
University of Aberdeen

Research Article

Keywords: low salinity, waterflooding, wettability, oil recovery, double-layer, geochemical reaction

Posted Date: March 16th, 2022

DOI: https://doi.org/10.21203/rs.3.rs-1455366/v1

Geochemical Numerical Simulation of Low Salinity Waterflooding in Sandstone Reservoirs

Oubai Elagab*
College of Engineering, Department of Petroleum and Natural Gas
University of Khartoum, Sudan
Email: oubaimishal@gmail.com

Abstract

In this paper, the underlying mechanisms behind the low salinity waterflooding were investigated. It has been ascertained that wettability alteration towards more water-wet is the leading cause to enhance oil recovery and observe the low salinity effect (LSE). The double-layer expansion mechanism has been considered the most probable reason for the wettability alteration due to low salinity waterflooding. Therefore, mechanistic modeling of low salinity waterflooding was approached by developing a diffuse layer surface complexation-based model that accounts for the double-layer expansion phenomena. The model was developed using the geochemical reaction path code PHREEQC, wherein the speciation and surface charge development at the oil-brine and kaolinite-brine interfaces were determined. Consequently, both the electrostatic pair linkages and the electrostatic forces were calculated, which led to predicting the qualitative change in the rock wetness owing to the low salinity effect. Wettability alteration owing to low salinity water flooding was predicted as a function of the oil composition, pH environment, ionic strength, divalent ions of the injected brine, and the concentration of the divalent cations in the formation water. The wettability change was qualitatively estimated using three approaches: bond product sum, zeta potential, and stability number.

Overall, the high levels of pH in the system and the high acid content in the oil composition proved to have a beneficial impact in observing the low salinity effect and thus wettability alteration towards more water-wet. In contrast, increasing the ionic strength and the divalent cation concentrations at both formation water and injected brine suppressed the low salinity effect. Also, the abundance of Ca^{+2} in the formation water was more pronounced than Mg^{+2} to suppress the LSE. The results also showed that the bond product sum approach could not predict the wettability alteration owing to low salinity waterflooding when the pH level is higher than five.

Keywords: low salinity, waterflooding, wettability, oil recovery, double-layer, geochemical reaction.

1. Introduction

Oil extraction from fluid reservoirs is an essential process in daily life. The need for energy is increasing as the population rises worldwide. Many researchers have stated that the energy demands will be increased significantly in the future. In its 2018 Outlook for Energy, ExxonMobil states that by 2040, a profound increment in the world population from 7.4 billion people to 9.2 billion is expected. This will be accompanied by the global Gross domestic product (GDP) growth to be double. All these factors will lead to a revolution in energy demand, and it is expected to increase by about 25% by 2040. Therefore, all economic energy sources will be needed to pursue to keep up with this considerable demand growth. Renewable energy sources such as wind and solar are expected to be the dominant sources of the energy supply in order to meet the need for energy. However, the oil is expected to keep growing and remain the primary energy source for transportation and chemical feedstock [1].

It can be concluded that increasing energy demand is maintained by hydrocarbon production. However, the economic feasibility of oil field development projects increasingly becomes under doubt as the oil price is decreasing [2]. So, there is a pressing need to produce oil from hydrocarbon accumulations in a cost-efficient manner to meet the global energy demand.

Throughout crude oil production from a reservoir, the system's embodied pressure continuously declines as fluid is extracted from it. This pressure is the primary driving mechanism that facilitates hydrocarbon extraction from the underground to the surface. However, upon progressive decline, the pressure deterioration eventually reaches levels at which its spontaneous drive does no longer satisfies the economic limit of production [3].

Waterflooding is commonly implemented by injecting water into the reservoir to boost production beyond the economic limit. This is primarily achieved by maintaining the pressure within the system and displacing the

remaining oil from the matrix towards producer wells. Thus, improving oil recovery. This process is regarded as a secondary recovery mechanism as it solely involves the injection of water/brine from injector wells into the reservoir without altering the rock-fluid properties [3, 4]. Water flooding performance is affected by different factors such as reservoir heterogeneity, residual oil saturation, and the quantity of injected water. In this regard, recent observations demonstrated that a higher increase in oil recovery factor is accomplished by manipulating the chemical composition of the injected water in a process termed low salinity water flooding (LSWF) [5, 6], smart water flooding [7], controlled salinity water [8], engineered water injection [9] and ions tuning water flooding [10]. Some experimental results showed a 34 % increase in oil recovery owing to LSWF compared to conventional water flooding [11], and a reduction of oil saturation by 9 % was observed in the field located in the North Slope of Alaska. However, some reservoir trials and laboratory studies failed to observe the low salinity effect (LSE) [6, 12, 13]. There is a common agreement that wettability alteration is the leading cause behind the LSE. However, the underlying mechanisms that lead to wettability alteration during LSWF are still debatable. The literature has proposed many mechanisms, including fines migration, increased pH effect and saponification, multi-component ion exchange, double layer expansion, organic compounds desorption from the rock surfaces, and the salt out effect [14].

The conventional water flooding wherein a similar composition of formation water is injected into a reservoir does not change the equilibrium condition within the hydrocarbon system. In contrast, lowering the salinity of the injected brine results in disturbing the stable chemical equilibrium state that induces the geochemical reactions in the crude oil/brine/rock (COBR) system; as a result, electrostatic repulsion forces are created between the oil and rock surfaces which in turns change the wettability in the system [13, 15].

Oil adhesion into the rock surface is occurred by different mechanisms, including the direct adsorption of the polarized acidic and basic oil compounds into the oppositely charged surface rock or by the presence of the divalent cations, which are served as a bridge that binding dissociated oil compounds -COO^- into negatively charged surface species exists at the rock surface. The wettability alteration is achieved by breaking the bridges between the oil compounds and the surface rock species which is induced by lowering the injected brine's salinity [16].

Mechanistic modeling approaches of LSWF vary from very simple to most complex models, and this primarily depends on the assumption used to derive the model. The earliest mechanistic modeling attempt was performed by Jerauld et al. (2008), who incorporate the LSE by relating the salt concentration and the oil recovery in a linear relationship wherein, the relative permeability curves move towards the water-wet conditions when the lower salt concentration is introduced into the system [17]. The mechanistic modeling of LSWF was further developed by incorporating the effect of the multi-component ion exchange reactions into a multi-phase reservoir simulator GEM^{TM}. However, some results are inconsistent with the model outputs [18]. Recently, an integrated model that accounts for the double-layer expansion mechanism has been approached by developing a surface complexation based-model through which the surface complexation reactions occurred at oil-brine, and rock-brine interfaces are introduced into the system using the geochemical reaction path code PHREEQC wherein the concentration of the surface species developed at the oil-brine and rock-brine interfaces is determined which are used to calculate the electrostatic pair linkages configured between the two interfaces, hence predicting the qualitative change in the rock oil wetness and the related oil desorption [15]. The surface potential at the oil and rock surfaces is also calculated using PHREEQC software to predict the wettability of the system, according to the DLVO theory the stability of the water film exists between the oil-brine and rock-brine interfaces is controlled by the charges developed at the oil and rock surface, the potential at the shear plane (zeta potential) is used to predict the surface potential at the interfaces which controls the stability of the water layer spread on the rock surface such as similar polarity of zeta potential at oil and rock surfaces create electrostatic attraction forces between the oil-brine and kaolinite-brine interfaces which lead to rupture the water film spreads on the rock surface while the same polarity of zeta potential results in a repulsive forces between the two interfaces and thereby enhancing the stability of the thin water film, meaning that inducing the wettability alteration, stable water film results in a water-wet condition which in turn lead to more oil desorption while the oil-wet condition is stablished when the water layer is unstable and therefore less amount of oil is released from the rock surface [19, 20].

According to the literature review, both laboratory experiments and field trials observed an increase in oil recovery owing to LSE. However, the primary mechanism behind LSWF is not clearly defined and still under debate. The complexity of the reactions that occur in the COBR system is the leading cause behind the less understanding of the LSE [18]. As a result, few mechanistic modeling attempts were initiated to simulate the process. Finally, the

computer Modeling Group company incorporated a new feature accounted for mechanistic modeling of LSWF in a 3-D reservoir simulator termed CMG- GEM wherein, multi-component ion exchange is considered as a primary mechanism behind the LSE while the surface complexation reactions were overlooked, as the results the model failed to observe some experimental results[18]. Since then, a pressing need to develop a commercial 3-D reservoir simulator incorporating such reactions has emerged. In this regard, efforts are extensively paid to capture this challenge, and few surface complexation-based models were developed without proper success in observing the LSE [19].

The number of site densities of acidic and basic compounds available at the oil-brine interface is taken as constant in most of the surface complexation-based models. However, the oil composition is an essential factor in determining the actual number of site densities that exist at the interface and could be one of the potential factors that lead to the failure of the developed models [21]. Therefore, a comprehensive understanding of the factors that affect the LSWF should be addressed to build a representative surface complexation-based model and coupled with a 3-D reservoir simulator to quantify the incremental oil recovery owing to LSE. Therefore, providing a tool to select a potential reservoir candidate for LSWF implementation.

This paper is aimed to investigate the effect of different factors on the degree of oil desorption during the LSWF process in sandstone reservoirs. The objectives can be summarised as follow:

- To investigate the underlying mechanisms behind the LSE in the COBR system.
- To identify the effect of the ionic strength and the divalent cations on the oil recovery factor during LSWF.
- To investigate the effect of the oil composition and pH level on the oil recovery factor.

A critical review of the underlying mechanism behind the LSE will be carried out. Then the impact of different parameters during LSWF will be addressed using a numerical modeling approach. In this regard, a surface complexation-based model should be built to incorporate the complex reactions that occurred in the COBR system during LSWF, and this is primarily achieved by specifying an appropriate configuration of the reactions that occur at the oil-brine and rock brine interfaces beside intra-aqueous reactions. A double layer model will be used to describe the interfacial region at the kaolinite-brine interface. After defining all the required parameters and specifying a detailed composition of the system's components, a code will be developed to simulate the low salinity waterflooding process in a geochemical reaction path PHREEQC. The developed code will be validated with the published experimental results and then used to analyze and predict the effect of different factors on the degree of oil desorption (recovery factor) owing to the LSE.

2. Literature Review

The quantity of oil recovered from a given reservoir can be increased using the water flooding process which is commonly implemented to boost the production beyond the economic limit, primarily by supplying the pressure to the system and displacing/sweeping the remaining oil from the matrix into the producer wells. Thus, improving oil recovery. It is regarded as a secondary recovery mechanism as it solely involves the injection of water/brine from injector wells into the reservoir without affecting the rock-fluid properties. Water flooding efficiency is affected by different factors such as reservoir heterogeneity, residual oil saturation, and different designing parameters, including the quantity of injected water. Recently it has been discovered that the quality of the injected water has a significant impact on the recoverable amount of oil [22]. Numerous experiments at the laboratory level and field trials have extensively shown that improved oil recovery can be achieved by altering the chemistry of the injected brine during water flooding. However, the primary mechanism behind the low salinity effect (LSE) is not clearly defined [8].

A. Low Salinity Water Flooding (LSWF)

The cost-effectiveness and the accessibility of the source water make the LSWF process serve as one of the best options among all practical methods to increase oil recovery. However, the significant role of the water composition in improving oil recovery has not been well highlighted until the experimental results of Morrow and his co-workers were published [6, 23]. Following that, extensive laboratory works have been conducted to address the effect of the LSWF; most of the results proved the increase in oil recovery factor when the salinity level of the injected brine was reduced in sandstone and carbonate rocks [24, 25]. British Petroleum Company implemented

extensive laboratory works at ambient and reservoir conditions to critically investigate the LSE, resulting in the registration of LoSal™ as a commercial enhanced oil recovery method [11, 26, 27]. Some experimental results showed a 34 % increase in oil recovery owing to LSWF [11], while the reduction in the residual oil saturation by 9 % was observed in the field located in the North Slope of Alaska. However, some reservoir trials failed to observe the LSE [6, 12]. This uncertainty suggests highlighting certain conditions under which LSE can be observed: the presence of clay mineral, presence of polar oil compounds, presence of initial water saturation, and presence of divalent cations in the initial water saturation [6]. Despite the proven effectiveness of the LSWF at both field trials and experimental works, the primary mechanism behind the LSE is still debatable, and many mechanisms have been proposed.

Proposed Mechanisms of Low Salinity Waterflooding

The underlying mechanism behind the LSE is not clearly defined. However, most of the suggested mechanisms are agreed on wettability alteration as being the leading cause of improving oil recovery. The most common mechanisms have been published in the literature are fines migration, Increased pH effect and reduced interfacial tension, a local increase in pH,multi-component ion exchange (MIE), and double-layer expansion [18].

Increased pH Effect and Reduce Interfacial Tension

Numerous studies at the laboratory scale have reported the increase in pH levels during LSWF [28, 29]. PH rise was ascribed to carbonate dissolution, which results in excess of OH^- in the aqueous liquid phase and subsequent increase in ph [28].

A considerable increase in pH above 9 in a subsurface hydrocarbon system can result in an alkaline-like enhanced oil recovery process, wherein the wettability alteration towards more water-wet is achieved by the generation of in-situ surfactant, which in turn decrease the interfacial tension between the oil and water [11, 30]. This mechanism is in doubt as being the primary mechanism of LSWF since there is no relation between the pH increase and the incremental amount of oil recovered [30]. Moreover, wettability alteration induced by alkaline flooding requires a high acidic number (AN> 0.2) to generate a sufficient amount of surfactant, while the highest experimental record of incremental oil recovered owing to smart water flooding was reported for oil's acid number less than 0.02 [30].

Fines Migration

Johnston and Beeson (1945) observed a significant permeability reduction, about 70 %, in 1200 oil sandstone core samples. They attributed the drastic decrease in permeability due to the flow of freshwater over the clay-bearing [31]. Many researchers have reported that the level of water salinity has a significant impact on permeability [31]. Bernard (1967) attributed the low salinity due to the swelling clay phenomena [32].

In 1999, Tang and Marrow performed numerous experiments on Berea sandstone cores containing clay as the main mineral constituent. They stated that during LSWF, some clay particles that previously adhered to the polar oil compounds are released and liberate some of the clay attached oil, leaving the pore walls exposed to more water-wet as shown in Fig. 1. This process results in increasing the amount of oil recovered [28]. Stripping clay particles process is controlled by the balance between two forces, namely: mechanical force and DLVO, the former is the net summation of the capillary force and the viscous force, while the latter combines both Van der Waals attraction forces and electrostatic repulsion forces. LSWF affects the equilibrium state within the system, increasing the electrostatic repulsive forces and the stripping process; therefore, more oil desorption is encountered [28].

The increase in oil recovery factor due to fines migration is supported by the observation of clay particles production and permeability reduction during LSWF. However, several experimental studies observed the LSE in the absence of clay particles production [33] or even permeability reduction [30]. Moreover, the increase in oil recovery in the carbonate rocks due to LSWF cannot be justified by clay particles migration [34].

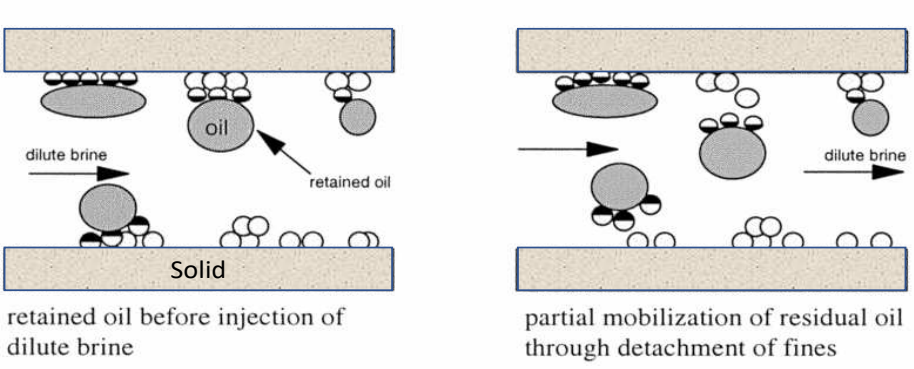

Fig. 1: Fine migration and clay-particles stripping mechanism [28].

local Increase in pH

Austad et al. (2010) proposed a mechanism by which oil desorbs from the clay surface due to the chemical reaction between the divalent cations adhered to the surface and hydrogen ions in the adjacent water layer. Austad and his co-workers consider the equilibrium condition at the initial state where both oil acid /base compounds and the divalent cations are attached to the surface rock. When the low salinity brine is injected into the system, the initial equilibrium state is disturbed due to a different composition of the injected brine; the system reaches a new equilibrium by replacing the calcium ions in the rock surface with the hydrogen ions from the adjacent water, and therefore, the pH level is increased and (OH-) ion reacts with the polarized acid and base oil compounds which results in oil desorption from the clay surface, and the more water-wet condition is established [12]. On the contrary, many experimental studies demonstrated the LSE with an even slight decrease in pH level, and there is no established correlation between the pH of the effluent and the LSE [35]. The representations of the proposed mechanisms for both acid and base reactions are depicted in Fig. 2.

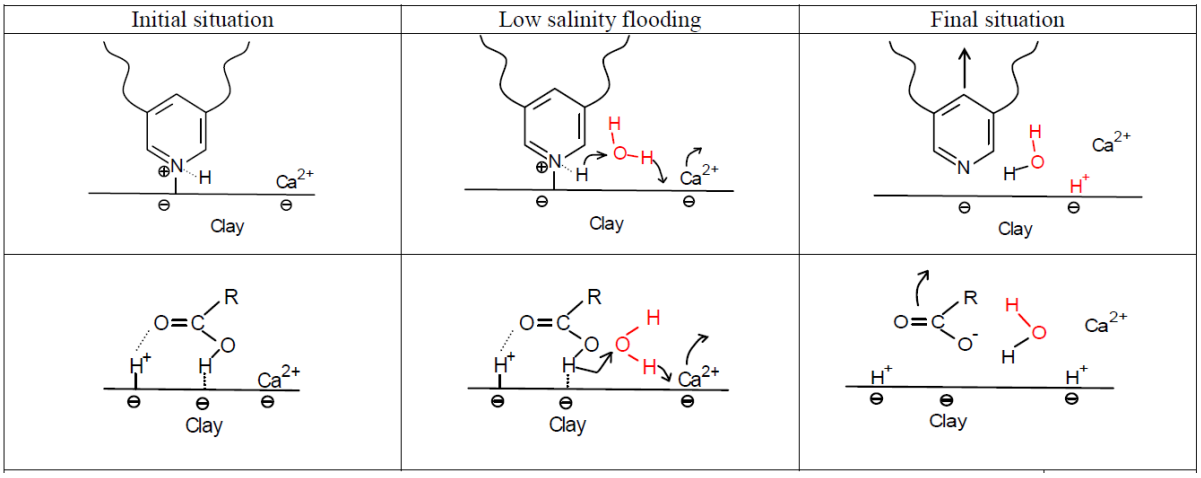

Fig. 2: Proposed mechanism for oil desorption under the effect of LSWF flooding. Upper: the basic oil component desorption Lower: the acidic oil component desorption. [12].

Multi-component Ion Exchange

The multi-component ion exchange mechanism was firstly noticed by Valocchi et al. (1981) when he observed a significant decrease in the concentration of the divalent cations (Ca^{+2}, Mg^{+2}) in the effluent during injection of freshwater into an aquifer system [36]. A better understanding of the process can be clarified after introducing the oil desorption mechanisms which are proposed by Buckley et al. (1998), who introduced four approaches by which oil adheres into the surface rocks as follow [16]:

- Interactions between the polarized components exist in the oil and the charged solids: Nitrogen basic compounds and carboxylic acids are the most common functional groups that undergo the chemical polarization process, as shown in Fig. 3. Generally speaking, the type of clay mineral, the amount of nitrogen

in the oil, and the solvent's quality in which the polar compounds are dissolved are some of the significant factors that influence the adhesion of polar compounds into the solid surfaces in the lack of water [16].

- Surface Precipitation: Oil quality is considered a decisive factor that determines its ability to control the precipitation process of their asphaltene components. So, poor oil quality results in more oil-wet, as described in Fig. 3.
- Acid-Based interactions: Mineral compounds can either gain negative charges when they donate a hydrogen ion (acid) or earn a positive charge when they receive proton (base), same as crude oil phase, which undergoes polarization process that results in both negative or positive charged surface group. The adhesion due to acid-base interaction illustrated in Fig. 3 as a negatively charged group at the mineral surface Si-O- (acid) is strongly adsorbed into a positively charged nitrogen compound (base) [16].
- The divalent cations such as Ca^{+2} in the formation water act as a bridge that strongly connects the negatively charged species in the mineral surface into the base/acid compounds at the oil phase, as illustrated in Fig. 3. It is worth noting that the presence of divalent cations masks the pure acid-base interaction adhesion mechanisms, which are relatively weak bonds in comparison with the bonds developed through the divalent cation's bridges [16].

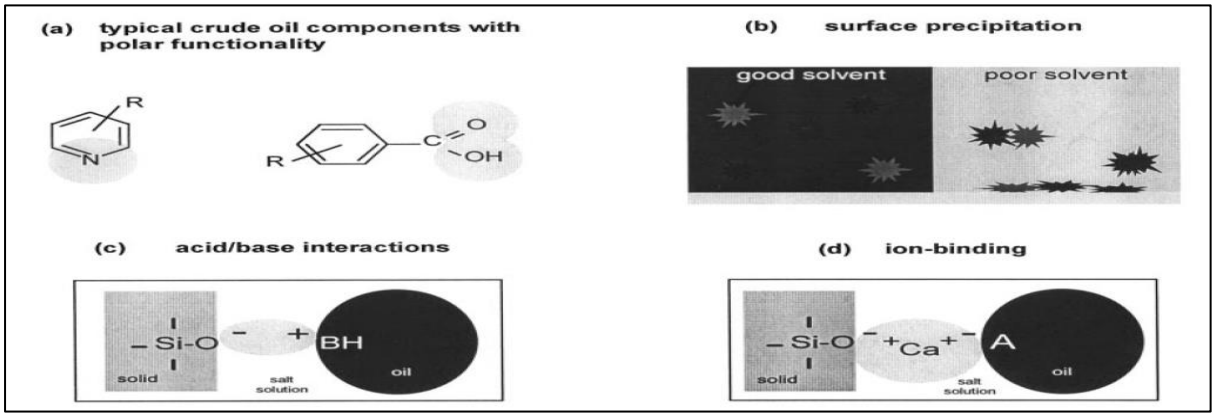

Fig. 3: Oil adhesion mechanisms in the solid surface [16].

The multi-component ion exchange mechanism occurs during LSWF by ions substitution that results in releasing the polar oil components and organometallic compounds from the mineral surface. This mechanism was experimentally investigated by Lager et al. (2008): a north slope core was firstly flooded at 25 °C by high salinity water, resulting in a 42 % recovery factor. Then, low saline water was introduced into the system in a tertiary mood, which produced 6% additional oil recovery. The second arrangement of the experiment was conducted at a reservoir condition (102 °C) where the core was flooded using high saline water, which resulted in a 35% oil recovery factor. Then the initial condition of the core was restored after stripping all the divalent cations from the rock surface by continuous flushing of NaCl. Thus, the organometallic complexes were removed due to the absence of the divalent cations. The injection of high saline water results in a 48 % oil recovery factor, while the tertiary flooding mood using Car-free low saline water produced no additional oil recovery. The core was then flooded using low saline water containing divalent cations with no increase in the oil recovery factor. The results imply that the LSWF induces substituting the divalent cations that were initially attached to the polar oil compounds. As a result, the organometallic complexes are desorbed from the surface, and higher oil recovery is obtained. This evidence proposed MIE as a primary cause behind the LSE [30]. The theory was latterly weakened by arguing that if a multi-ion exchange is a primary mechanism behind the LSE, it should be more pronounced in minerals with high cation exchange capacity (CEC) instead of being correlated with kaolinite which has low CEC [30].

Electrical Double Layer (EDL) Expansion

It is generally assumed that a thin water film separates the oil-brine and mineral-brine interfaces in the COBR system. According to the DLVO theory, the stability of the water film is controlled by the intermolecular interaction forces between the two interfaces, namely: Van der Waals forces, structural forces, and electrostatic forces [37]. The charge's distribution at both oil and rock surfaces play a significant role in the electrostatic forces

in a way that similar polarities at both oil and rock surfaces create a repulsive force between the oil-brine and rock-brine interfaces, leading to the expansion and stabilization of the thin water film that exists between the two interfaces. In contrast, when opposite polarities are developed, the attraction force is induced, resulting in an unstable water film, which results in more oil adhering to the rock surface and less water condition being established. The ionic strength of brine plays a critical role in the system by screening off the charges/potentials at both oil and rock surfaces. The higher ionic strength of injected-brine neutralizes more charges at both oil and rock surfaces and reduces the electrostatic repulsive forces between the two interfaces. As a result, the stability of the thin water layer between the two interfaces might be ruptured. In contrast, low ionic strength has less potential to screen off the charges at the oil and rock surfaces, which yield a more stable water film between the oil/brine rock/brine interfaces. Based on this theory, Ligthelm et al. (2009) proposed that the primary mechanism behind LSE can be justified by the expansion of the thin water film spread on the rock surface. The LSWF implies low ionic strength and, therefore, high zeta potentials, which indicates the surface potential at both oil and rock surfaces are created. The higher zeta potential magnitudes result in higher electrostatic repulsive forces, which in turn lead to wettability alteration in the system towards less oil-wet condition [22]. However, a further decrease in the ionic strength might have a detrimental impact on oil recovery. For instance, the repulsive forces exerted on clay particles can exceed the critical coagulation force that binds the clay particle to each other. Thus, clay sheets undergo a stripping process, resulting in formation damage in the hydrocarbon system, and less oil recovery is achieved [28]. The LSE owing to double layer expansion is observed when the ionic strength is decreased by reducing the concentration of the divalent cation [20, 28]. On the contrary, the results obtained from the quartz surface test wherein the increase in oil desorption was achieved by increasing the level of salinity at a constant pH. Furthermore, the double-layer expansion mechanism failed to demonstrate the LSE in some cases [8].

B. Geochemical Reactions in COBR System

The COBR system includes the formation water, reservoir rock, oil, and injected water. The LSE is observed due to several geochemical reactions that occur within the system when ionically tuned water is injected into a reservoir. These reactions are aqueous speciation, mineral dissolution/precipitation reactions, ion-exchange reactions, and surface complexation reactions. Aqueous reactions occur fast and within one phase, hence commonly assumed as an equilibrium reaction. In contrast, the components involved in mineral dissolution reactions are in different phases; hence, they are considered heterogeneous reactions. The ion exchange reactions commonly occur between the clay and ions present in the brine [9].

Surface complexation reactions incorporate the interaction between aqueous and surface functional groups and consider the electrical interfacial region theory as well. The activity coefficient for each surface species is corrected in these reactions by incorporating the detailed description of the electrical interfacial region where the ion-sorption reactions occurred. It has been highlighted that during surface complexation reaction, the developed-surface charges affect the constant equilibrium of the surface reaction mass law. Therefore, an additional exponential term was introduced to modify the intrinsic equilibrium constant. So, the adapted constant includes two terms: the exponential term, which accounts for the electrostatic forces developed by the surface charges, and the original term accounts for the ion-sorption reaction (intrinsic equilibrium constant), the reaction is expressed by [38]:

$$K_s = K_{int}.exp\left(-\frac{zF\Psi}{RT}\right) \quad (1)$$

Where K_s, K_{int} is the equilibrium constants for the aqueous solution and the intrinsic, respectively, z is the valence, F is the Faraday constant, Ψ is surface potential, R is the universal gas constant, and T is the absolute temperature. An important parameter used for surface complexation reactions calculations is the ionic strength of the solution. The ionic strength represents the amount of salt in an electrolyte and is calculated by:

$$I = 0.5\sum_{i=1}^{n} c_i z_i^2 \quad (2)$$

Where c_i represents the concentration of ion i and z is its valence number.

C. Mechanistic Modeling Approaches of Low Salinity Waterflooding

Despite the complexity of COBR system and less understanding of the underlying mechanisms behind the engineered water Injection, mechanistic modeling of LSE is increasingly demanded to quantify the incremental oil recovery from a given reservoir under certain conditions. Hence, provide a decision-making tool for screening oil fields under development schemes [39]. There is a common agreement that wettability alteration is the leading cause behind LSE. Therefore, the mechanistic modeling of designed water flooding based on wettability alteration can be incorporated into the model by changing wettability-dependent properties such as relative permeability and capillary pressure characteristics as well as residual oil saturation [40].

The first attempt in modeling approaches to demonstrate the LSE is developed by Jerauld et al. (2008), wherein the salt is considered as a single additional component in the aqueous phase, and total dissolved solids (TDS) is used as a control parameter for wettability alteration. Jerauld and his co-workers assigned two values for each relative permeability curve, capillary pressure curves and residual oil saturation, where the two values represent the high salinity case and low salinity case. The linear interpolation between the two cases is used to predict the correspondent wettability-dependent properties as a function of total dissolved solids. Firstly, they defined the residual oil saturation as a function of brine salinity and used this as an interpolant to estimate the modified sets of relative permeability curves and capillary pressure curves at each salt concentration [17, 40]. Their model failed to match the experimental measurements due to overlooking the complex reactions that occur in the system during LSWF. However, it provided a starting point for further modification and development of LSWF models.

Advanced mechanistic modeling of LSWF was demonstrated by Omekeh et al. (2012), who incorporated the multi-component ion exchange mechanism (MIE) in their model to simulate the LSWF in a sandstone rock. Wettability alteration is accomplished by altering the relative permeability curve owing to divalent cation release from the clay surface as a result of multi-ion exchange reactions. The release of divalent cations such as calcium and magnesium from the clay surface is induced by LSWF, which results in oil desorption and an increase in oil recovery. The model findings were in a better agreement with the experimental results compared to the previous models [41].

A more detailed model that incorporates aqueous reaction, mineral dissolution/precipitation, and multi-component ion exchange were developed by Dang et al. (2013); the integrated model was built in the geochemical package PHREEQC and coupled with a multi-phase compositional simulator GEM™. The interpolant used to modify the relative permeability curves is a function of the equivalent fraction of ions adhered to the rock surface. The developed model was examined by reproducing the experimental data conducted on a series of North Sea core floods; the results reasonably matched the experimentally measured data [42]. Both previous models were developed considering multi-component ion exchange as a primary mechanism during LSWF without relevance of the ionic strength effect [39].

A more comprehensive geochemical-based model coupled with a compositional reservoir simulator is developed by Korrani et al. (2016), wherein the complex geochemical reactions occur in the crude oil/brine/rock system were captured in the geochemical code PHREEQC while the effect of the multi-phase flow was considered in a 3-D compositional reservoir simulator UTCOMP developed by the University of Texas. The new feature incorporated into the UTCOMP_IPHREEQC model is the solubility effect of oil's component on the recovery factor. The authors highlighted that the solubility of the CO2 results in a significant change in a system's pH level, which in turn controls the LSE. Korrani and his co-workers considered the expansion of the electrical double layer as the primary mechanism behind the LSE. Thus, they used the total ionic strength as the interpolation parameter in their developed model [43]. The output of the UTCOMP_IPHREEQ model matched the experimental core floods measurement obtained by Kozaki (2012). However, the model failed to observe the effect of the divalent cations during LSWF [44]. Since then, the surface complexation models have increasingly received attention to serving as a comprehensive tool to select the potential reservoir candidates for engineered water flooding.

D. Electrical Double Layer Theory

Electrical double-layer theory is used as a base for all surface complexation models. This section presents the theory and the models developed to describe the electrical double layer.

Electrical Double Layer Models

According to his model, the electric double layer theory was first introduced by Helmholtz in 1897: two charged layers with different polarities are developed at the interface between a charged electrode and an electrolyte

solution. Fig. 4 is an illustration of the Helmholtz model as he considered the charged electrode attract counter ions while co-ions are repelled away, the two layers are separated by a distance equal to the radius of the counterions. The concept of the sharp decline in the potential between the two layers was improved by Gouy and Chapman (1913) by considering the motion of the ions under the influence of the thermal agitation and the electrostatic forces, which results in a so-called diffuse layer, as shown in Fig. 4, according to their model: the thickness of the diffuse layer extends some distance towards the bulk solution, and the ions are treated as point charges. Moreover, the electrical potential is gradually declined and governed by the Poison-Boltzmann equation [45]. The EDL model was further modified by Stern (1924), who improved Gouy-Chapman's model by considering the layer of adsorbed ions, in other words, stern theory based on considering both the fixed Helmholtz layer where the counter ions are adsorbed into the charged-electrode and the diffuse layer where the motion of ions are induced by thermal diffusion and the electrostatic forces as shown in Fig .4 [46, 47].

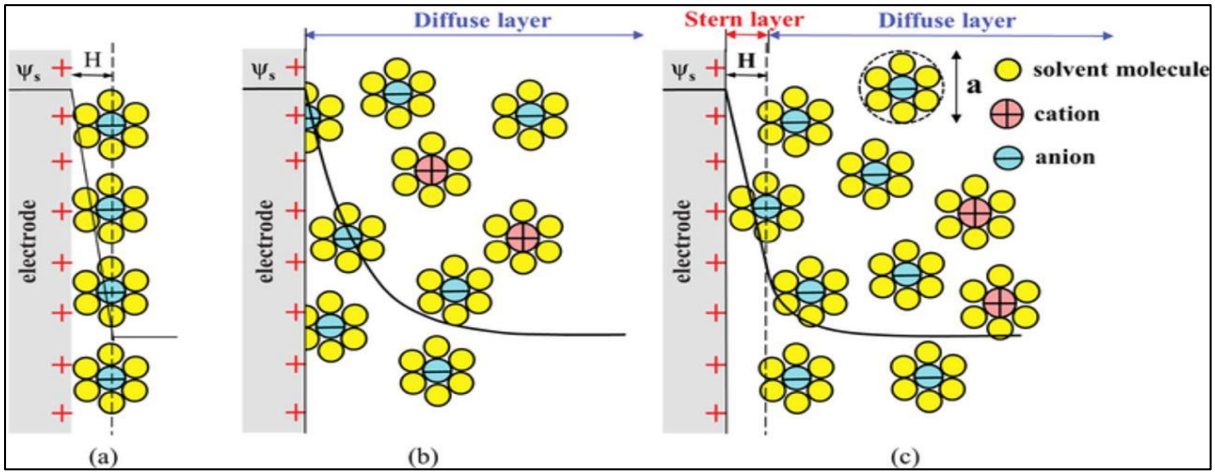

Fig. 4: Electrical double layer models with the distribution of the counter ions and co ions at the electrolyte/solution interface [47].

Surface Potential Development

In the electrical interfacial layer depicted in Fig. 5, the rock surface is made up of different concentrations of protonated surface sites, deprotonated surface sites, and neutral surface sites based on the pH level that prevails in the system. In a typical reservoir condition, the negative sites dominate the overall charge. Therefore, the counter ions from the electrolyte solution are attracted into the solid surface: some of the counterions are strongly adsorbed into the rock surface, forming the stern layer where the ions are adsorbed into the rock surface and fixed. The adsorbed counter ions in the stern layer are not enough to screen off all the negative charges at the rock surface. Thus, excess positive ions diffuse in the diffuse layer where the ions loosely adhere to the surface via coulombic force. The abundance of counterions in the diffuse layer decreases exponentially with distance in the direction of the bulk solution until the neutral electrical charge is encountered. When the system is induced by external energy such as pressure gradient, the bulk solution together with part of the diffuse layer is moved, and a disturbance of the neutral charge conditions in the system is encountered, creating a streaming potential in the system. The boundary between the mobile and immobile parts of the diffuse layer is termed the shear plane, and the potential at this plane is called the zeta potential, which can be experimentally measured [48, 49] and can also be used to calculate the potential at the surface. It is worth noting that the thickness of the stern layer is relatively small compared to the diffuse layer, as illustrated in Fig. 5. However, a significant potential drop occurs within the stern layer.

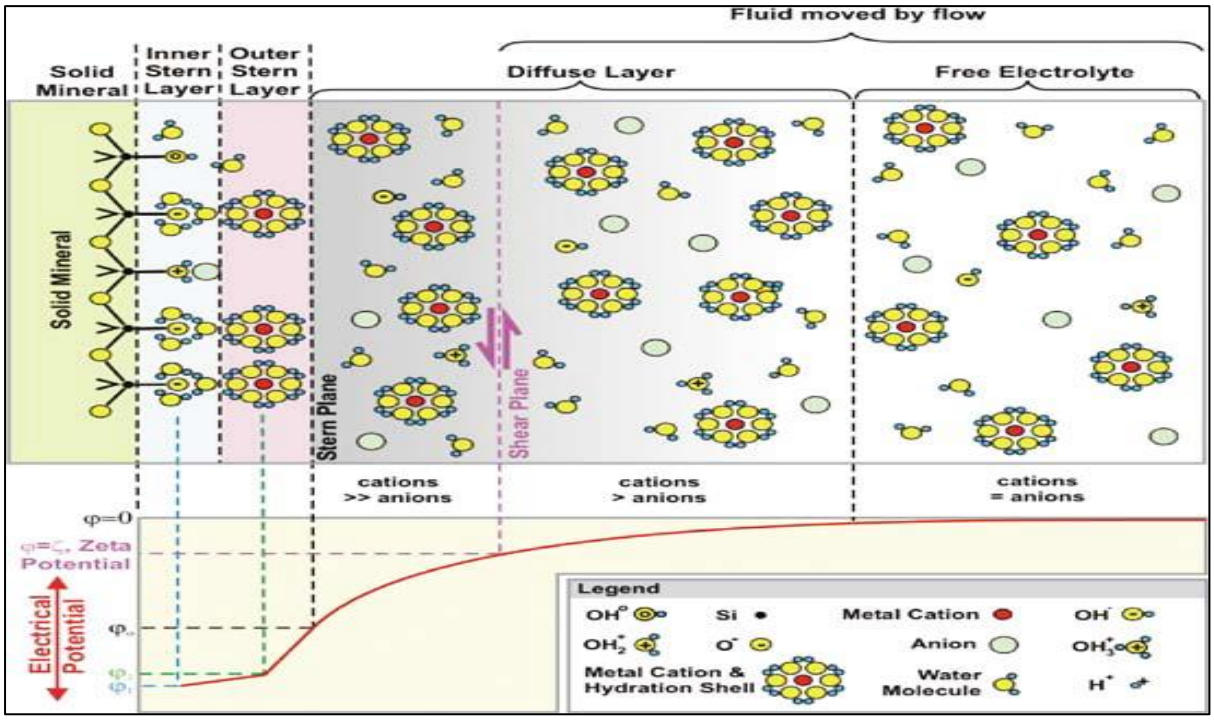

Fig. 5: Electrical double layer at the rock -brine interface [49].

E. Surface complexation Modeling

A surface complexation model is an approach used to describe ions sorption onto mineral surfaces by incorporating the interaction between aqueous and surface functional groups as well as the electrical interfacial region theory. The activity coefficient for each surface species is corrected in the SCM by incorporating the detailed description of the electrical interfacial region where the ion-sorption reactions occurred [38, 50, 51]. Brady and krumhansl (2012) stated that Models of surface complexation make it possible to model the charge distribution on both oil and mineral surfaces based on the composition of the injected brine [52]. The main challenges with SCMs are providing a detailed description of ion sorption in the electrical interfacial region, identifying different types of surface functional groups at the rock surface, formulating reaction stoichiometry of the surface complexes, and finally using an efficient technique to estimate the model's input parameter [50, 51].

Sandstone Surface Reactivity

The mineral composition of the clastic rocks depends on the deposition environment under which rocks are formed. The mineralogical constituents of the sandstone reservoir contain several types of minerals such as quartz, feldspar, oxide coating, and carbonate [53].

Clay minerals have the highest reactive surface area observed by oil because of their small grain size, sheet morphology, and much larger surface area. The surface area dominated by clay minerals is 100 to 1000 times much higher than that occupied by quarts or feldspar on a weight basis. However, the bulk surface area of the sandstone might not be dominated by clay in excessively clean sandstone that contains less than 1% clay by weight [53]. The approximate ranges of the reactive surface area of clay minerals are 10 to 38 m2/g (kaolinite), 65 to 100 m2/g (illite), and 600 to 800 m2/g (montmorillonite), while quartz and feldspar have a surface area of 0.1 m2/g [54].

Types of Surface Complexation Models

The differences among surface complexation models mainly arise from their capability to describe the electrical interfacial region and the location of the ion adsorption with respect to the surface across a broad spectrum of conditions. Including more details on the model provides a more accurate and realistic description of ion sorption and desorption. However, the disadvantage of detailed SCMs is that the description of surface-ions interactions requires a comparatively large number of parameters that cannot be accurately achieved and consequently affects the uncertainty of the model. The most common types of surface complexation-based models are the constant capacitance model, diffuse layer model, triple-layer model, and charge distribution multi-site surface

complexation model. The constant capacitance model is considered as a particular case for the diffuse layer model [38].

Diffuse layer model

The diffuse layer model was firstly proposed by Schinder et al. (1968) and Stumm et al. (1970), who investigate the interactions at the oxide edge that lead to ions -sorption into the oxide surface. They highlighted that the reactions result in forming charges at the oxide surface, which affect the constant equilibrium of the surface reaction mass law. Therefore, an additional exponential term was introduced to the equilibrium constant. So, the adapted constant includes two terms: the exponential term, which accounts for the electrostatic forces created by the surface charges, and the original term, which accounts for the sorption reaction. The electrostatic term was derived by Schinder et al. (1968) and Stumm et al. (1970) from the base of the electrical double layer theory by considering two layers at the oxide water interface: the first layer represents the oxide surface while the second one is a diffuse layer which contains counter ions. The presence of a solution with high ionic strength was assumed by Schinder and his co-workers, which resulted in developing a constant capacitance between the two layers, while Stumm used Gouy-Chapman equation (GCE) to describe the diffuse layer in the interfacial electrical region. GCE is derived by assuming the low ionic strength of a solution. In conclusion, the distinction between the two models is how the diffuse layer is incorporated into the model, as depicted in Fig. 6. However, the model developed by Shinder and his co-workers has been termed the constant capacitance model (CCM), while Stumm's et al. model is known as a diffuse layer model (DLM) [38].

In the diffuse layer model, all the ions are adsorbed into the solid surface, and the model can be developed by adapting four parameters, including the equilibrium constant for protonation, deprotonation, and metal adsorption reactions, as well as the site density (NS), which is determined by the availability of sites number per mass of solids as sites/nm^2. The relation between the electrostatic potentials and the surface charge density (σ_d) is controlled by Gouy Chapman equation as follow:

$$\sigma_d = -01774 \,.\sqrt{I}\,.\sinh\left(\frac{z\,F\,\psi_d}{2\,R\,T}\right) \tag{3}$$

Where z is the valence of the ion, F is the Faraday constant, R is the ideal gas constant $(j/K.mole)$, T is the absolute temperature (K), ψ_d is the electrostatic potential of the layer d.

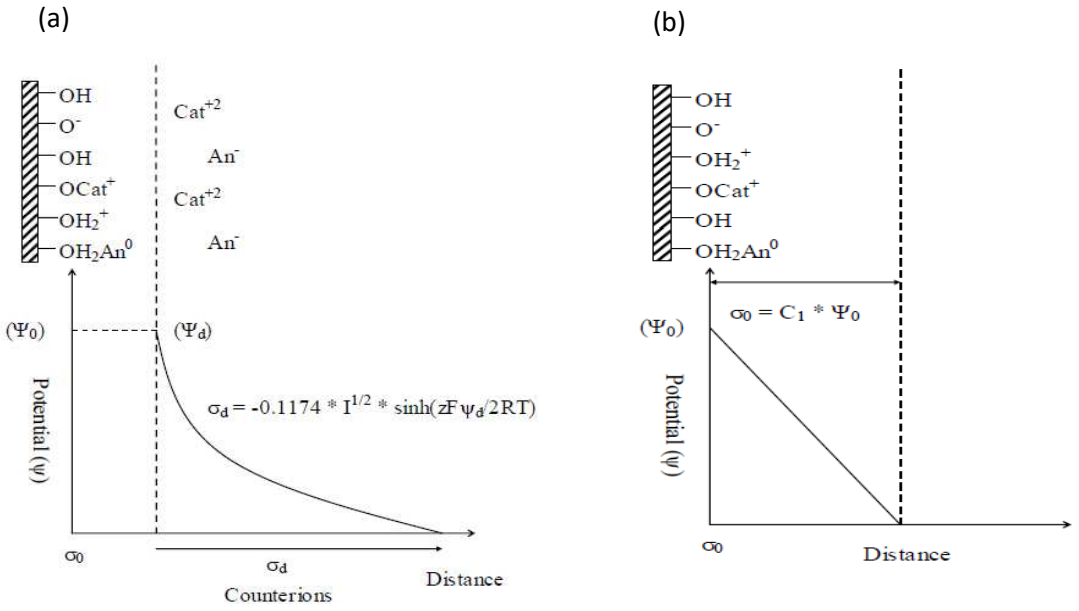

Fig. 6: Representation of the electric double layer (EDL) used in (a) the diffuse layer model [51].

Triple-layer model

Triple-layer model proposed by Davis and refined by Hayes and Leckie (1986) wherein a detailed description for ions adsorption is captured. For instance, strongly bound ions such as H+ & OH- are allocated in a plane very close to the surface. However, the loosely bound ions are placed in another plane. They also consider a diffuse layer for the motion of the other ions [55].

1.1.1 Mechanistic Modeling Using Surface complexation Models (GR)

Brady and krumhansl (2012) developed a surface complexation model using the geochemical package PHREEQC to determine the concentrations of the charged surface groups at the kaolinite and oil surfaces. The concentration of charged groups at the kaolinite edge are [> Al: Si-O-], [> Al-O-H2+], and [> Al:Si-O-Ca+] while the charged surface group at the oil surface are [-COOCa+], [-NH+] and [-COO-]. The product of oppositely charged group from both oil and kaolinite surfaces form the electrostatic pair linkage [> Al:Si-O-][-NH+], [> Al:Si-O-][-COOCa+], [> Al-O-H2+][-COO-], [> Al:Si-O-Ca+][-COO-] as shown in Fig. 7. The sum of the electrostatic pair linkages is termed Bond Product Sum (BPS), which is used as a predictive tool for wettability alteration during engineered water injection. The BPS provides a description of the degree of oil adhesion into the rock surface. For instance, higher BPS means higher electrostatic attraction forces between the oil and kaolinite surface groups, which results in the less water-wet condition.

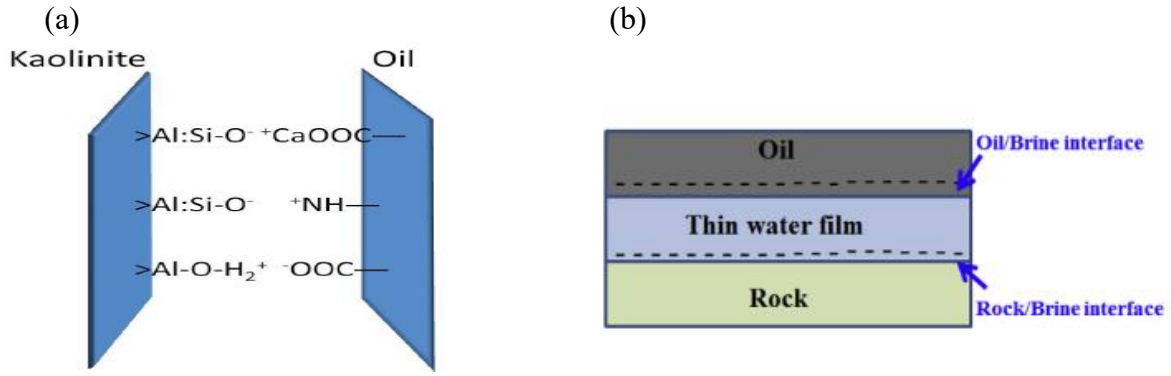

Fig. 7: a) Oil sandstone electrostatic pair linkages b) the thin water film between oil-brine and rock-brine interfaces [44, 52].

Samuel Erzuah (2017) developed a surface complexation model using PHREEQC, where different mineralogical constituents (Kaolinite, quartz, calcite) were considered, and the effect of the oil composition was accounted. The attractive electrostatic pair linkage between the oppositely charged surface groups at the oil and rock surfaces was calculated for the three minerals at different divalent cations concentrations. The PBS and the surface charges at the oil-brine and rock-brine were determined and used as a qualitative wettability-prediction tool. The results were compared with the contacts angles derived from their corresponding flotation test, which emphasize the outputs achieved by the surface complexation model [56].

Elakneswaran et al. (2017) developed an integrated surface complexation model using geochemical path reaction code PHREEQC, where in kaolinite-bearing sandstone was assumed to dominate the rock's surface reactivity. Mineral dissolution and precipitation are incorporated into the model as a new feature from the previous models. The wettability alteration is predicted by quantify the percentage of oil desorption as a function of the injected-brine composition. The oil desorption is calculated based on the concentration of surface functional groups at both oil and kaolinite edges. Elakneswaran and his co-workers claimed that the equilibrium phases of mineral reactions significantly affect the model's output. Their results demonstrate that oil desorption is achieved during LSWF. However, the great LSE was observed when calcium concentration was decreased. In addition, more oil desorption was achieved when mineral equilibrium phases were considered [57].

Korrani and Jerauld. (2019) Developed an integrated surface complexation based-model using a geochemical package code PHREEQC coupled with the reservoir simulator UTCOMP to capture the multi-phase flow. The model accounted for aqueous reactions, surface complexation reactions, and oil acid-base contents. In their work, the wettability alteration is modeled by defining a dimensionless parameter termed stability number (SN), which is derived based on comparing the competition between the repulsion and attraction forces act on the thin water

layer that exists between the oil-brine and rock-brine interfaces. For stability numbers higher than one, the electrostatic repulsive forces between the two surfaces dominate the intermolecular forces within the system, and therefore, the stable water film is established. In contrast, the domination of Van der Waals attraction forces (SN < 1) leads to rupturing the thin water film and consequently leads to less water-wet conditions [44]. The electrostatic force is induced by the charge development at both oil and rock surfaces and can be quantified using zeta potential values. The model was validated using experimental data published by Kozaki (2012) and the reported observations of the LSE of Endicott field trial [56].

Takeya et al. (2019) claimed that a surface complexation model that describes the electrical interfacial region using a diffuse layer model could not predict zeta potential magnitudes at different brine compositions. Therefore, they developed a triple-layer surface complexation-based model in which the potentials can be directly measured at different planes. The model was developed using a geochemical reaction path PHREEQC and the parameters for the model were dependently measured and validated by the experimental published data [19].

F. Wettability Alteration

Wettability alteration is related to reservoir geochemistry through the concept of disjoining pressure as defined by the DLVO theory, which is concerned with intermolecular forces within a colloid [44]. A thin water film spreads on the mineral surface that separates the oil ad rock in a crude oil-brine-rock system. The stability of the thin water film is controlled by the intermolecular forces, which acts on the two interfaces, i.e., oil/brine interface and brine/rock interface, which in turn play a significant role in altering the wettability of the system [37].

The study of the ionically tuned water flooding effect at a nano-scale has been conducted by Hirasaki (1991), where it was claimed that wettability alteration within the COBR system is controlled by the stability of the thin water film. The term "disjoining pressure," which is defined in the DLVO theory, was used to quantify the stability condition of the thin water film [44]. The disjoining pressure is defined as follows:

$$\Pi_{Disjoining\ Pressure} = \Pi_{Van\ der\ Waals} + \Pi_{structural} + \Pi_{electrical} \quad (4)$$

Where Π indicates the intermolecular force between the oil/brine and rock/brine interfaces, a positive disjoining pressure indicates the domination of the electrostatic repulsion forces between the oil-brine and rock-brine interfaces which leads to expanding and stabilizing the thin water film between the two interfaces. This stabilization results in water-wet conditions prevailing in the system. A negative disjoining pressure indicates the domination of attraction forces between the two surfaces, which leads to rupturing the thin water layer in the system, i.e., unstable conditions, and therefore, less water-wet condition is encountered. The disjoining pressure is the summation of three different intermolecular forces: Van der Waals forces, structural forces, and electrostatic forces, which are developed due to the interaction between the two interfaces in the COBR system. A brief explanation of these three forces on the disjoining pressure and the consequence wettability alteration is discussed below:

Van der Waals Forces

It is always an attractive force between two particles and classified to either weak London dispersion force or strong dipole-dipole intermolecular force. Van der Waals forces contribute negatively to the disjoining pressure and act on disturbing the stability of the thin water. For a constant ionic strength and water film thickness, Van der waals force is a function in Hamaker constant which is strongly affected by the temperature [37].

Electrostatic Forces

This force results from the development of charges at both oil and rock surfaces as a consequence of protonation, deprotonation, and cation adsorption reactions which occur at the rock-brine interface as well as the polarization of acid/base compounds at the oil-brine interface. The electrostatic forces between the two interfaces can contribute either positively or negatively to the disjoining pressure term based on the polarity between the two interfaces. Similar polarities at both oil/brine and rock /brine interfaces create repulsive electrostatic forces, while oppositely charged surfaces result in creating an attraction force between the two surfaces. The electrostatic force between the oil and rock surfaces is related to the potential surfaces, which is immeasurable. Therefore, zeta potential, which is the potential at the shear plane - zeta potential - is used instead [37].

Structural Forces

In comparison with van der Waals forces and the electrostatic forces, the structural forces are considered a short-range reaction for a distance less than 5 nm between the oil/brine and rock/brine interfaces. It has a positive share in the disjoining pressure [38].

DLVO theory predicts the wettability alteration by defining the disjoining pressure, as mentioned before. Hirasaki (1991) defined the oil adhesion/non-adhesion boundary to describe the oil-wet and water-wet regions for a given COBR system by comparing the electrostatic repulsion forces and the Van der Waals attraction force [44].

Korrani and Jerauld (2019) introduced a dimensionless group termed the Stability number, which is a ratio between the electrostatic repulsion forces and the attraction forces to describe the wettability alteration during LSWF. Brady (2015) proposed a parameter called Bond Product Sum (BPS) wherein the sum of electrostatic pair linkages (the product of oppositely charges surface species concentrations at both oil and rock surfaces) is used as a predictive tool for wettability alteration [15].

Experimentally, Jackson et al. (2016) developed a correlation between the oil recovery factor and the measured zeta potential at both water-brine and mineral-brine interfaces. Their work concluded that improved oil recovery could only be observed when manipulating the chemistry of the injected water in a way that provides the same polarity of zeta potential at both oil-brine and mineral brine interfaces [34].

3. Methodology

A. Model Overview

Mechanistic modeling of low salinity water flooding was developed by reproducing a surface complexation-based model for an integrated crude oil/brine/rock system proposed by Brady and Krumhansl (2012). The model was built by developing a code in the geochemical path reaction code PHREEQC. The model captured the intra-aqueous speciation, surface-aqueous equilibrium phases, and surface complexation reactions between rock, oil surfaces, and aqueous solution. In this work, the effect of the oil composition was accounted for, and the advection process of injected brine is simulated as a new feature to the original model.

The surface complexation reactions at both oil-brine and rock-brine interfaces as well as the formation water composition, were defined, then the equilibrium condition was established. The injected brine was introduced into the system. Therefore, different interactions were induced to reach a new equilibrium state. A diffuse layer surface complexation model was utilized to account for the speciation and surface charges development at both oil-brine and rock-brine interfaces. The concentrations of the surface species were used to calculate the bond product sum which is used to evaluate the wettability alteration. The surface charge density was used to determine the surface potentials at the two interfaces, which were also used to predict the wettability alteration. It is worth mentioning that the potential at the shear plane (Zeta potential), which is measurable, is always used instead of surface potential to predict the wettability conditions in the system. The calculation of zeta potential from the surface potential is achieved using Debye-Huckel approximation Eq. (26) or Gouy-Chapman solution Eq. (28) based on the potential values as will be explained in the mathematical model. Furthermore, the location of the shear plane is adjusted within the range of 0.2 nm up to 2 nm according to the ionic strength following other studies [21]. A brief illustration of the developed model steps is shown in Fig. 8.

The built-in PHREEQC surface complexation model can be either based on Dzombak and Morel (1990) model or the charge distribution multi-site model (CD-MUSIC). The database for the former model was derived from the complexation reactions of heavy metal ions on hydrous ferric oxide where the surface potentials are correlated to the surface charge through Gouy-chapman equation (diffuse layer model) while the latter allows ion sorption at different layers (e.g., stern layer and Helmholtz layer). Therefore, the potentials can be estimated with reasonable accuracy at different planes [58].

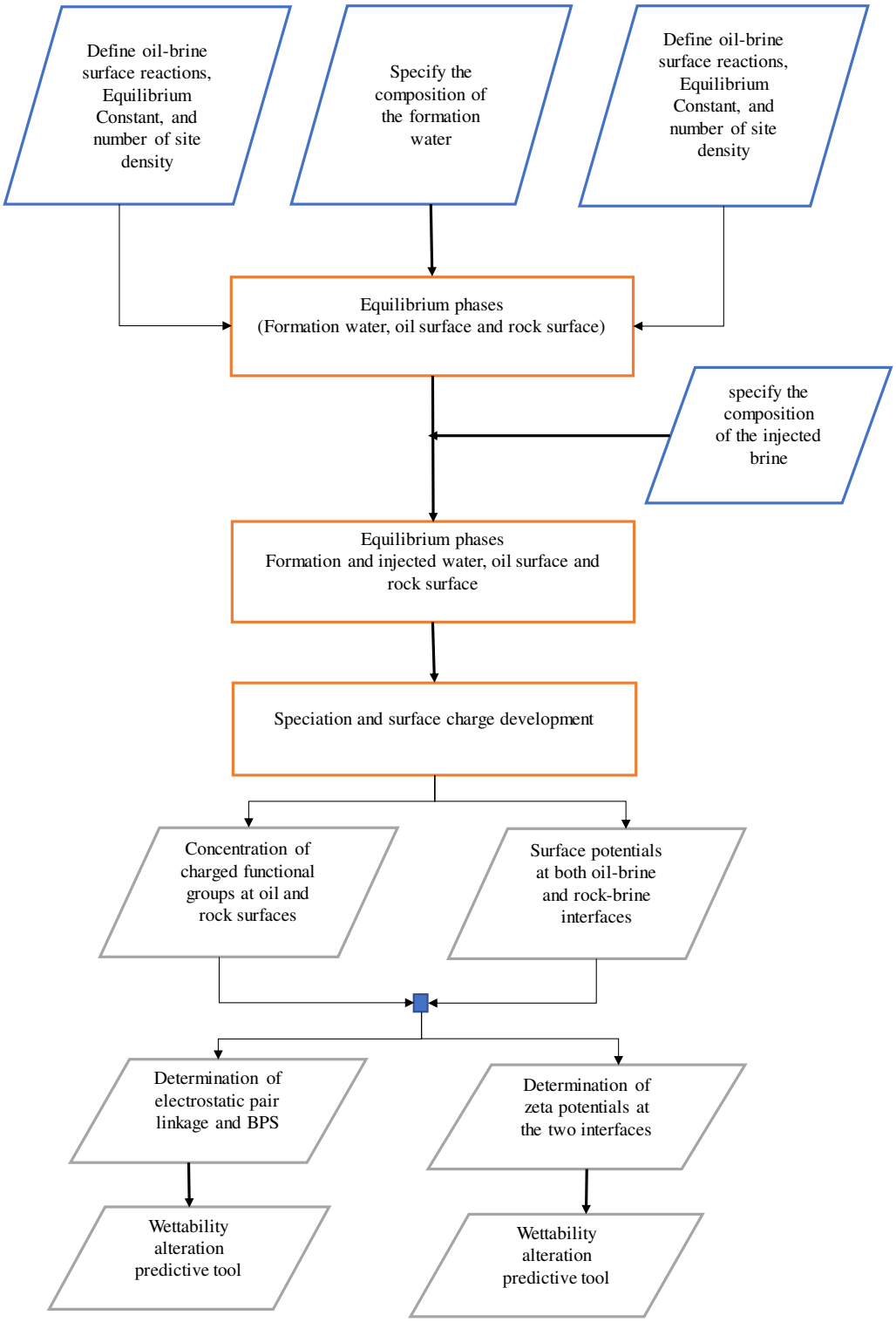

Fig. 8: Illustration of the steps used to predict the wettability alteration using SCMs.

B. PHREEQC

PHREEQC is an open-source geochemical reaction model instructed using C++ programming language commands. The geochemical package PHREEQC was developed by the United States Geological Survey (USGS) to model the complex interactions that occur within the groundwater system. The model can process various interactions between water and minerals, gases, ion exchangers, surface complexes, and solid solutions. The equilibrium reactions are defined by non-linear equations as an optimization problem that is iteratively solved

using the Newton-Raphson technique [59]. The non-linear equations to be resolved are brought from the database containing equations in the form of standard chemical mass action form. Kinetic reactions are formulated in ordinary differential equations terms and then solved explicitly or implicitly [60].
Different types of processes can be handled using PHREEQC geochemical path reaction code, including speciation and saturation index calculation, equilibrium phases calculation,1-D transport reversible/irreversible calculation, and inverse modeling calculation [58].
PHREEQC model input data can be categorized into three types of keywords. Firstly, system specifying commands such as SOLUTION_SPECIES, MASTER_ SOLUTION_SPECIES, SURFACE_SPECIES, GAS PHASE, and SOLID_SOLUTIONS. Secondly, manager commands such as PRINT, TITLE, USE, END, SAVE, SELECTED_OUTPUT, and SOLUTION_SPREAD. Finally, Batch reaction commands are used to perform an action such as SOLUTION, REACTION, MIX, SURFACE, ADVECTION, INVERSE_MODELING, EXCHANGE, EQUILIBRIUM_PHASES, KINETICS [61].

C. Model Development

Developing a code in PHREEQC

To develop the surface complexation model, three types of command blocks were used: system specifying commands, manager commands, and batch reaction commands. This code was used to model the complex crude oil/brine/rock system interactions. It is worth noting that **phreeqc.dat** database file was amended by adding the oil surface properties and the corresponding surface complexation reactions to make it possible to model the COBR system. Different keyword blocks were used to develop the model. A batch reaction file was set using the following keywords:

TITLE	Used to describe the model under the process (e.g., low salinity water flooding)
SOLUTION	Used to define the chemical composition of aqueous solutions at a specified temperature, pH level, and density.
SURFACE_MASTER SPECIES	Used to identify the surface sites at both oil and kaolinite surfaces and their corresponding master surface species.
SURFACE SPECIES	Used to define the surface complexation reactions that occurred at the oil-brine and kaolinite-brine interfaces, including protonation, deprotonation, and divalent cation sorption interactions
SURFACE	Used to define the chemical composition of surfaces assemblage in terms of number of site density and specific surface area.
EQUILIBRIUM_PHASES	Used to control a constant level of pH during batch reactions by adding some NaOH to react with an aqueous solution if needed.
SAVE	Used to save the output of the batch reaction to use it later
USE	Used to select specified solution or surface to be incorporated into the current batch reaction
ADVECTION	A command is used to allow the flow of injected brine into the system, which results in replacing high salinity formation water
END	To end the batch reaction simulation.

Model Input Data

Four parameters were used to define the diffuse layer surface complexation based-model; $K_{Me}^{int}, K_{+}^{int}, K_{-}^{int}, N_s$ where the first three terms represent the equilibrium constants for metal adsorption, protonation, and deprotonation reactions, respectively, while the last term indicates the site density, which is the number of sites per unit surface area available for proton exchange [62]. In addition, the surface area, which is defined by the unit mass of the solid available for liquid /gas phase [38] is also required to build the model. The

composition of the formation water and the injected water, along with the temperature, are vital as well. The reactions at both oil and rock surfaces are described in detail in the following subsections.

Oil Surface Modeling

The surface charge at the oil-brine interface is modeled by considering nitrogen bases and carboxylic acids as the functional surface groups at the oil edge. The positive charges develop from the polarization of weak nitrogen bases linked to heterocycle aromatic groups, while the negative charges arise from the polarization of the carboxylic acids [52]. The site density for both carboxylic acids and nitrogen bases functional groups are estimated to be the same and equal to 1 site/nm^2 based on the electrokinetic measurements conducted on the bitumen/water interface [63].

The protonation and deprotonation reactions occur at the oil-brine interface as well, as the coordination of the divalent cation Ca^{+2} with carboxylate oil surface group is modeled as observed at the bitumen/water interface [52] and are expressed as:

$$-NH^+ \leftrightarrow -N + H^+ \qquad K_1 = \frac{[-N]a_{H+}}{[-NH^+]}\exp\left(\frac{F\Psi}{RT}\right) \tag{5}$$

$$-COOH \leftrightarrow -COO^- + H^+ \qquad K_2 = \frac{[-COO^-]a_{H+}}{[-COOH]}exp\left(\frac{F\Psi}{RT}\right) \tag{5}$$

$$-COOH + Ca^{2+} \leftrightarrow -COOCa^+ + H^+ \qquad \mathrm{K_3} = \frac{[-\mathrm{COOCa^+}]\mathrm{a_{H+}}}{[-\mathrm{COOH}]}\exp\left(\frac{-\mathrm{F\Psi}}{\mathrm{RT}}\right) \tag{7}$$

Where $-COOH$ and K_{-COOH} are the dangling carboxylate and nitrogen base groups present at the oil–water interface $[-COOH]$ and $[-COO^-]$ represent the surface concentrations ($\mu mol/m^2$), F is Faraday's constant, Ψ is the surface potential, a_{H+} represents the activity of the hydrogen ion , R is the universal gas constant and T is the absolute temperature.

Sandstone Reservoir Surface Modeling

Clay minerals dominate the sandstone reactive surface area due to their small grain size, sheet morphology, and much greater surface area. The surface charge at the rock-brine interface can be modeled by considering protonation, deprotonation, and divalent cations sorption at the kaolinite oxide surface as follows:

$$> A1 - O - H_2^+ \leftrightarrow > A1 - O - H + H^+ \qquad K_4 = \frac{[> Al - O - H]a_{H+}}{[> Al - O - H_2^+]}\exp\left(\frac{F\Psi}{RT}\right) \tag{8}$$

$$> A1 - O - H \leftrightarrow > A1 - O^- + H^+, \qquad \mathrm{K_5} = \frac{[> \mathrm{Al - O^-}]_{\mathrm{a_{H+}}}}{[> \mathrm{Al - O - H}]}\exp\left(\frac{\mathrm{F\Psi}}{\mathrm{RT}}\right) \tag{9}$$

$$> Si - O - H \leftrightarrow > Si - O^- + H^+, \qquad K_6 = \frac{[Si - O^-]_{a_{H+}}}{[Si - O - H]}\exp\left(\frac{F\Psi}{RT}\right) \tag{10}$$

$$> Al{:}Si - O - H + Ca^{2+} \leftrightarrow > A1{:}Si - O - Ca^+ + H^+ \qquad K_7 = \frac{[> Al{:}Si - O - Ca^+]a_{H+}}{a_{Ca2}[> A1{:}Si - O - H]}\exp\left(\frac{-F\Psi}{RT}\right) \tag{11}$$

$$> Al{:}Si - O - H + CaOH^+ \leftrightarrow > Al{:}Si - O - CaOH + H^+ \qquad K_8 = \frac{[> Al{:}Si - O - CaOH]_{a_{H+}}}{a_{CaOH+}[> Al{:}Si - O - H]}\exp\left(\frac{-F\Psi}{RT}\right) \tag{12}$$

Where $Al - O$ and $Si - O$ represent Al and Si edge sites.

The model set the surface area for both oil and rock surfaces was set as 10 m^2/g in the model. The summary of the reactions that occur at both oil and kaolinite surfaces, along with their equilibrium constants, are shown in Table 1 [52].

Table 1: Base case surface complexation modeling parameters at 100 °C

Reaction	25°C $\log K$	Enthalpy (KJ/mol)	Site density $(\mu mol/m^2)$
Oil – Water Interface			
$-NH^+ \leftrightarrow -N + H^+$	-6.0	34	$-N$: 1.67, $-COO$ 1.67
$-COOH \leftrightarrow -COO^- + H^+$	-5.0	0	
$-COOH + Ca^2 \leftrightarrow -COOCa^+ + H^+$	-3.8	1.171	
Kaolinite edges			
$> Al - O - H_2^+ \leftrightarrow > Al - O - H - H^+$	-3.0	0	
$> Al - O - H \leftrightarrow > Al - O^- + H^+$	-3.8	32	
$> Si - O - H \leftrightarrow > Si - O^- + H^+$	-7.0	32	$> Al$: 1.92, $> Si$: 1.92
$> Al - O - H + Ca^{2+} \leftrightarrow > Al - O - Ca^+ + H^+$	-9.7	45	
$> Si - O - H + Ca^{2+} \leftrightarrow > Si - O + Ca^+ + H^+$	-9.7	45	
$> Al - O - H + CaOH^+ \leftrightarrow > Al - O - CaOH^+ + H^+$	-4.5	45	
$> Si - O - H + CaOH^+ \leftrightarrow > Si - O - CaOH + H^+$	-4.5	45	

D. Model Assumptions

- The surface reactivity of the sandstone rock is dominated by clay minerals, and this is true except for excessively clean sandstone where the contribution of the clay into the rock minerals does not exceed 1% on a weight basis [52]. Furthermore, the kaolinite-clay bearing is the only type of clay considered in the study.
- The presence of pure kaolinite is considered; hence basal exchange reactions, which is caused by the heterovalent substitution in the lattice, were neglected [52].
- The equilibrium constants for surface complexation reactions are considered equal to their analog reactions in the bulk solution. For instance, the equilibrium constant for carboxylic acid speciation at the oil surface was set as equivalent to the dissolved mono-carboxylate [15]
- The polarization of acidic and basic oil components located at the oil-brine interface can be represented by the ionization chemical reaction process to model the oil-brine interface [64].
- Ions distribution in the diffuse layer model can be described using Gouy-Chapman equation (GCE), wherein the ions are treated as point charges, and the interactions between them are neglected. Hence, GCE can be used to correlate the surface charge density and the surface potential as a function of the ionic strength. The equation is assumed to be applicable for ionic strength up to 0.2 M.
- The analytical solution for the Poisson-Boltzmann equation proposed by Gouy-Chapman for 1:1 electrolyte is applicable for mixed electrolytes where NaCl dominates the solution
- The location of the shear plane is a function of the ionic strength ranging from 0.2 nm for high ionic strength up to 2 nm for low ionic strength [21].
- Mineral dissolution and precipitation reactions are not considered, and mineral surface complexation equilibrium constants were estimated from potentiometric titration measurement [15].
- During the advection process, the formation water originally exists in the system can be fully replaced by the injected brine [58].

E. Mathematical Modeling for the Diffuse Layer Model

The potential variation (ψ) through the diffuse layer can be expressed using Poison equation:

$$\nabla^2\psi = -\frac{\rho}{\varepsilon\varepsilon_0} \tag{13}$$

Where ρ is the chrge density in the system (in the unit of C/m^3), ε is the dielectric constant of the medium and ε_0 Is the permittivity of the free space.
By considering a single dimensional problem in x-direction which is acting vertically on the rock-brine interface, the expression of potential distribution within a diffuse layer is simplified into:

$$\frac{d^2\psi}{dx^2} = -\frac{\rho}{\varepsilon\varepsilon_0} \tag{14}$$

In the diffuse layer there will be an abundance of counterions. So, the demanded work to approach the counterion from infinity (bulk solution) to the position where the electrical potential value is ψ can be determined by $z_i e\psi$ where $z_i$is the valence number of i^{th} ion. The distribution of ion concentration within the diffuse layer is governed by Boltzmann series as

$$n_i = n_i^{\infty} \exp\left(-\frac{z_i e\psi}{kT}\right) \tag{15}$$

Where n_i is the number of ions of type i per unit volume close to the solution-surface interference, n_i^{∞} is the number of ions of type i per unit volume in the bulk solution, and e is the electronic charge.

While The charge density ρ can be correlated to ion concentration n_i by :

$$\rho = \sum_i z_i e n_i = \sum_i z_i e n_i^{\infty} \exp\left(-\frac{z_i e\psi}{kT}\right) \tag{16}$$

Therefore, the variation of the surface potential is ψ as a function of distance through the diffuse layer can be expressed by joining equations (3.2) and (3.4)

$$\frac{d^2\psi}{dx^2} = -\frac{e}{\varepsilon\varepsilon_0}\sum_i z_i e n_i^{\infty} \exp\left(-\frac{z_i e\psi}{kT}\right) \tag{17}$$

The derived equation Eq. (17) is widely used in different engineering applications and termed Poisson − Boltzmann equation, Poison-Boltzmann equation is a non-linear differential equation and cannot be used in its general form to determine the surface potential at different locations within the diffuse layer. Therefore, the analytical solution is achieved at a certain case by considering some boundary conditions. The most common analytical solutions for poison-Boltzmann were proposed by Debye − Hückel and Gouy-Chapman which are explained in detail below:

Debye − Hückel Approximation

By taking the Maclaurin series the exponential term in Eq. (17) can be extended into:

$$\exp\left(-\frac{z_i e\psi}{kT}\right) = 1 - \frac{z_i e\psi}{kT} + \frac{\left(\frac{z_i e\psi}{kT}\right)^2}{2!} - \cdots \tag{18}$$

Debye − Hückel approximation is applicable when the developed surface potential meets the condition $\left|\frac{z_i e\psi}{kT}\right| < 1$, the implication of that is, this analytical solution can only apply for small values of potential.

By considering the first and the second terms in the Maclaurin series and ignoring the rest terms Eq. (18) become:

$$\exp\left(-\frac{z_i e\psi}{kT}\right) \approx 1 - \frac{z_i e\psi}{kT} \tag{19}$$

By applying this approximation Eq. (16) can be expressed as:

$$\rho = \sum_i z_i e n_i^{\infty}\left[1 - \frac{z_i e\psi}{kT}\right] \tag{20}$$

The neutral condition within the bulk solution gives:

$$\sum_i z_i e n_i^{\infty} = 0 \tag{21}$$

From Eqs. (3.16) and (3.17)

$$\rho = -\frac{1}{kT}\sum_i z_i^2 n_i^\infty e^2 \psi \tag{22}$$

By calling the expression of charge density ρ from Eq. (22) into Eq. (14), The equation can be simplified in to:

$$\frac{d^2\psi}{dx^2} = \frac{1}{\varepsilon\varepsilon_0 kT}\sum_i z_i^2 n_i^\infty e^2 \psi \tag{23}$$

Equation (23) is the linear solution for poison-Boltzmann which is achieved by $\text{Debye} - \text{Hückel approximation}$.

To make further simplification, $\text{Debye} - \text{Hückel constant, k,}$ can be defined as :

$$k^2 = \frac{e^2}{\varepsilon\varepsilon_0 kT}\sum_i z_i^2 n_i^\infty \tag{24}$$

Then linearized Poison Boltzmann Eq. (23) can be further minimized by considering $\text{Debye} - \text{Hückel constant}$

$$\frac{d^2\psi}{dx^2} = k^2\psi \tag{25}$$

Now, we are going to consider two boundary conditions to solve Eq. (25) as follow:

$$\text{Condition 1: } x \longrightarrow 0\,, \qquad \psi \longrightarrow \psi_0$$

$$\text{Condition 2: } x \longrightarrow \infty\,, \qquad \psi \longrightarrow 0$$

Then the potential variation within the diffuse layer can be expressed as a function of distance as follow:

$$\psi = \psi_0 \exp(-kx) \tag{26}$$

Eq. (26) is the final representation of the analytical solution of poison-Boltzmann equation proposed by $\text{Debye} - \text{Hückel}$, the equation predicts an exponential decline profile for the potential magnitude ψ as going towards the bulk solution in the direction of $x \longrightarrow \infty$.

This equation is used to estimate the potential at the shear plane (zeta potential) at, the location of x is strongly affected by the ionic strength of the system and located within the diffuse layer.

The $Debye - Hückel\ parameter, k,$ has a unit of m^{-1}. The $Debye - length, k^{-1},$ can be calculated from the following equation.

$$k^{-1} = \left[\frac{NA^{e^2}}{\varepsilon\varepsilon_0 kT}\sum_i z_i^2 c_i^\infty\right]^{(-1/2)} \tag{27}$$

Which c_i^∞ is the concentration of ions of type $i,$ expressed in mol/m^3

Gouy -Chapman Analytical Solution

The applicability of $\text{Debye} - \text{Hückel}$ approximation is limited to low potential values. This limitation has been solved by Gouy-Chapman who introduced a general solution for poison Boltzmann equation for symmetrical electrolyte such as NaCl, the formulation simplified to

$$\psi_x = \frac{2kT}{e}\log\left[\frac{1+\gamma e^{-kx}}{1+\gamma e^{-kx}}\right] \approx \frac{4kT}{e}\gamma e^{-kx} \tag{28}$$

Where $\gamma = \tanh(e\psi_0/4kT)$

Eq. (28) Is a Gouy-Chapman analytical solution for 1:1 electrolyte and is used to predict the potential at the shear plane (zeta potential) when the surface potentials exceed 25 mV.

The mathematical model was adapted from [65, 66].

F. Model Validation

Generally, the surface complexation models are validated by comparing the calculated potential at the shear plane (zeta potential) with the measured values [66]. In this work, two surface complexation codes were separately developed using geochemical reaction path code PHREEQC to model the interfaces of oil-brine and rock-brine.

Oil-brine Interface

A diffuse layer surface complexation model was built to predict the published results reported by Buckley et al. (1989), wherein, zeta potential for the crude oil emulsion ST-86-1 was measured at different aqueous ionic strength 0.001, 0.01, and 0.1 M. The input parameters of the base case were used while the oil surface properties

were taken from the reported experimental data. The number of surface site densities were calculated from the reported acid and base number using Eq. (29) & Eq. (30) which results in 0.6 site/nm^2, 0.03 site/nm^2 for carboxylic acid and nitrogen bases respectively, the mass of oil and water used in the experiment were 0.004 g and 0.1 g accordingly. Moreover, the experiment was conducted at the ambient temperature 25^o C [67].
The surface potential at the oil-brine interface was calculated as a function of pH using the diffuse layer model in PHREEQC. Then zeta potential was predicted from the surface potential using either Debye-Hückel approximation Eq. (26) or Gouy-Chapman analytical solution Eq. (28) based on the surface potential magnitude. The location of the slip plane was used as a fitting parameter to match the data. It worth noting that the location of the shear/slip plane where zeta potential is measured is a debatable issue and there is no reference value that can be used. However, a range from 0.2 nm to 2 nm is frequently considered in the literature [21].

Kaolinite-brine Interface

A surface complexation model was developed to predict the published results observed by Nasralla and Nasr-El-Din (2014) where in, zeta potential for a kaolinite mineral with different NaCl concentrations 2, 10 and 50 g/l was measured at pH level 4.13, 4.17 and 4.4 respectively. the input parameters for the base case were used and the mass of the water and solid used in the experiment were incorporated into the model (10 g of kaolinite per 1 kg of water). The experiment was run at temperature 77 F [68]. The surface potential at the mineral-brine were determined using a diffuse layer model in PHREEQC as mentioned before, and then compared with the measured values.

G. Factors Affecting Wettability Alteration During LSWF

The wettability alteration during LSWF is affected by many factors. However, the investigation was conducted to address the effect of the pH, ionic strength, divalent cation level/type in the formation water and the injected-brine, and the oil composition. The sensitivity analysis was performed at each case by flooding different water composition to observe the change in wettability conditions in compare with the conventional water flooding where the high salinity formation water is injected.
The speciation and the concentration of the surface charged groups at the oil and rock surfaces are calculated at different pH levels as a function of ionic strength, divalent cations level and the oil composition. Then, both the electrostatic pair linkage and zeta potential are determined to address their effect on the oil adhesion.

Study of the pH Effect

The effect of the pH was investigated at different ionic strength, divalent cation concentration, and oil composition. The surface complexation model was built as a pH-dependant model such that each effect has been studied with varying pH levels. However, the detailed investigation of the pH effect was conducted by flooding a low salinity water into the system.

Study of the Ionic Strength Effect

The ionic strength is defined by Eq. (2) which demonstrates a proportional relation of the ionic strength with both molar concentration and squire root of the valency of ions makeup the solution. To address the effect of the ionic strength during low salinity water flooding, three water composition with different ionic strength were flooded into a hydrocarbon system where the high salinity formation water is in equilibrium with the oil and rock surfaces. The composition of the three injected brines are shown in Table 2, it should be noted that the high salinity formation water (HSFW) was flooded into the system as a conventional water flooding. A code was built to model the system by using the following key word blocks in PHREEQC: TITLE, SOLUTION, SURFACE_MASTER SPECIES, SURFACE SPECIES, SURFACE, EQUILIBRIUM_PHASES, SAVE, USE, ADVECTION and END**.**

Table 2: Composition of the injected brine at different ionic strength

Solution	Element	Con, mol/l	Ionic Strength, M
HSFw	Na	0.2	0.23
	Cl	0.22	
	Ca	0.01	
LS1	Na	0.1	0.115
	Cl	0.11	

LS2	Ca	0.005	0.056
	Na	0.05	
	Cl	0.054	
	Ca	0.002	

Study of the Divalent Cation [Ca^{+2}] Effect in the Injected-brine

To investigate the effect of the divalent cation concentration, calcium ions concentration in the injected brine is decreased from LS_1 to LS_2, and then totally removed from LS_3 while the ionic strength is kept constant, as shown in Table 3. Each brine composition was separately flooded into the reservoir, having a formation water HSFw to predict the wettability alteration as a function of divalent cation concentrations at different pH values.

Table 3: Composition of the injected brine at different divalent cation concentrations.

Solution	Element	Con, mol/l	Ionic Strength, M
HSFw	Na	0.2	0.23
	Cl	0.22	
LS1	Ca	0.01	0.095
	Na	0.08	
	Cl	0.09	
LS2	Ca	0.005	0.095
	Na	0.082	
	Cl	0.1	
LS3	Ca	0.002	0.095
	Na	0.095	
	Cl	0.095	

Study of the Divalent Cation [Ca^{+2}, Mg^{+2}] Effect in the Formation Water

To study the effect of the divalent cations that are inherently present in the reservoir, three different compositions of formation water (FW_1, FW_2, FW_3) with different divalent cations types and/or concentrations but the same ionic strength was separately flooded with a low salinity brine as shown in Table 4.

Table 4: Composition of the formation water at different divalent cation concentration/type

Solution	Element	Con, mol/l	Ionic Strength, M
LSWF	Na	0.01	0.01
	Cl	0.01	
FW1	Na	0.1	0.115
	Cl	0.11	
FW2	Ca	0.005	0.115
	Na	0.102	
	Cl	0.12	
FW3	Ca	0.002	0.115
	Na	0.1	
	Cl	0.11	
	Mg	0.005	

Study of the Oil Composition Effect

The amount of acidity and basicity at the oil-brine interface were used to incorporate the effect of the oil composition on the wettability alteration occurred during LSWF. The total acid number (TAN) and total base number (TBN) were linearly correlated to the oil surface site density available for proton exchange and divalent cations sorption. These reactions directly affect the surface charge developments and therefore the oil adhesion into the rock surface [21]. The correlation between acid/ base contents and surface site density is given by

$$N_{s,-COOH} = 0.602 \cdot 10^6 \cdot \frac{TAN}{1000 \cdot a_{oil} \cdot MW_{KOH}} \quad (29)$$

$$N_{s,-NH} = 0.602 \cdot 10^6 \cdot \frac{TBN}{1000 \cdot a_{oil} \cdot MW_{KOH}} \quad (30)$$

Where $0.602 \cdot 10^6$ is the factor to convert from $[mol/m^2]$ to $[\#/nm^2]$, $N_{s,-COOH}$, $N_{s,-NH}$ are the carboxylic acid and nitrogen base surface sites TAN $[mg\ KOH/g\ oil]$ is the total acid, while TBN $[mg\ KOH/g\ oil]$ is the total basic number, a_{oil} $[m^2/g]$ is the specific area of oil and MW_{KOH} is the molecular weight of potassium hydroxide $[g/mol]$.

To investigate the effect of oil chemistry, a range of selected acid and base contents were converted into their corresponding surface site density as shown in Table 5. the model was set as previously described with changing the number of oil site density for both carboxylic acid and nitrogen bases. The speciation, surface charge development and zeta potential were determined to address the effect of the oil chemistry on the oil adhesion in the hydrocarbon system.

The ionic strength of formation water and injected brine were 0.23 M, 0.12M respectively. The code was developed using the key words blocks: SOLUTION, MASTER_SURFACE_SPECIES, SURFACE_SPECIES, EQUILIBRIUM PHASES and ADVECTION.

Table 5: Oil composition with different acid/base contents

TAN $[mg\ KOH/g\ oil]$	TBN $[mg\ KOH/g\ oil]$	$N_{s,-COOH}$	$N_{s,-NH}$	TAN/TBN
1	0.5	1.073	0.537	2
0.5	0.5	0.537	0.537	1
0.05	0.5	0.054	0.537	0.1

H. Wettability Alteration Assessment Methods

The Bond Product Sum (BPS), Zeta Potential (ZP) and Stability Number (SN) were interchangeably used to predict the qualitative change in the wettability which reflects the degree of oil desorption from the rock surface and hence the oil recovery factor.

The BPS is a measure of the electrostatic attraction force developed between oil and rock surfaces, the determination of the BPS based on summing up all the products of surface concentration of oppositely charged functional groups exist at the oil and rock surfaces. Therefore, the higher BPS indicates higher electrostatic attraction forces between the oil and mineral surfaces which results in less water wet condition, while the PBS is equal to zero when all the charged surface species at both oil and rock surfaces have similar polarity and the water wet condition is prevailed. This method cannot be used to predict the wettability alteration during LSWF in the system with pH higher than 5.7 [15].

Zeta potential (ZP) is a measure of the potential at the slip plane created by the surface charge development, the electrostatic repulsion force is induced by the development of similar polarity of zeta potential at both oil and rock surfaces, the higher zeta potential values the stronger electrostatic repulsion force and therefore less oil wet

condition is encountered. While the attraction force is created between the two surfaces when opposite polarity of zeta potential is encountered, and the oil wet condition is prevailed [19].
The stability number (SN) is the ratio between the electrostatic repulsion forces and Van der Waals attraction forces which control the stability of the thin water film exist between the oil-brine and rock-brine interfaces. For SN above one, the higher SN the greater electrostatic repulsion forces between the interfaces and less oil wet condition is encountered However, the stability number less than one indicates the domination of the Van der Waals attraction forces and the oil wet condition is prevailed [44]. The mathematical expression for the SN given by

$$SN = 0.09\varepsilon_r^{1.5}\psi_{Oil/Brine}\psi_{Brine/Rock}\sqrt{\frac{T}{I}} \qquad (31)$$

It is worth noting that wettability alteration towards less oil condition occurs within a specified range limited by the minimum value of stability number above which wettability condition is changed towards water wet (SN_{min}) and maximum value of stability number above which no further wettability alteration can take place (SN_{max}) [44]. Unfortunately, there is no clear criteria have been stated by the authors on how to calculate the minimum and maximum stability numbers. However, the wettability alteration in this paper has been analyzed qualitatively without a pressing need to determine these values.

4. Results and Discussion

A. Model Validation

Oil-brine Interface

The model output was validated with measured zeta potential values for crude oil emulsion reported by Buckley et al. (1989). The electrolyte used in the experiment is NaCl with three different ionic strengths, 0.001 M, 0.01 M, and 0.1 M. the experiment input data was clearly explained in the methodology section. In this regard, it is worth noting that the total base number of the oil used in the experiment was not reported. However, it has been drawn from a recent study reported by Bonto et al. (2019), who inferred the base number from the correlation between the isoelectric point and the acid/base site density [21]

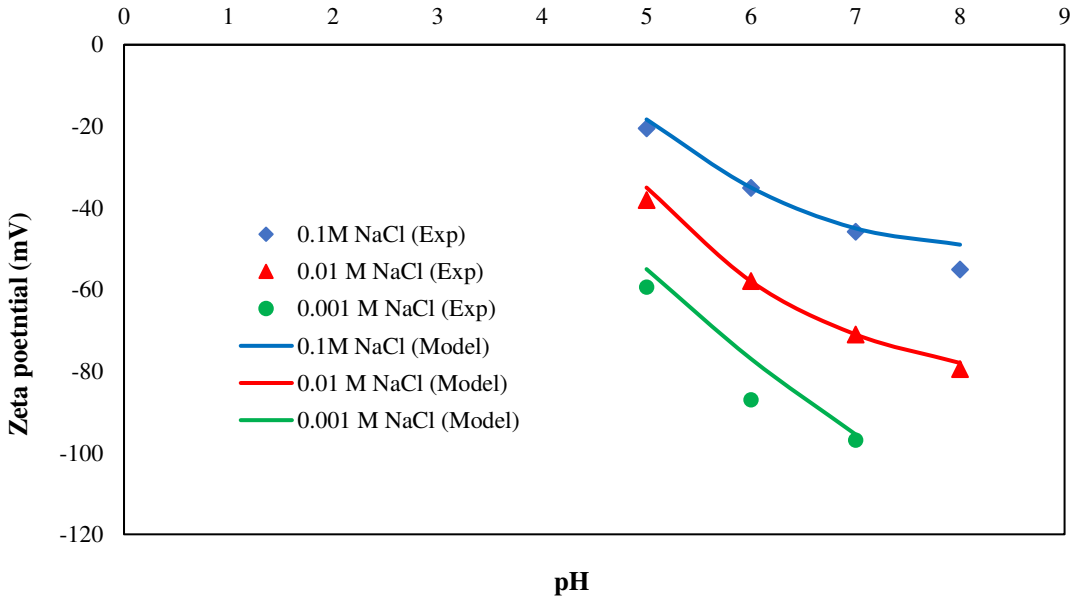

Fig. 9: Measured zeta potential at the oil-brine interface compared with the PHREEQC output.

Fig. 9 demonstrates the model capability of simulating measured zeta potential magnitudes in different ionic strengths 0.001 M, 0.01 M, and 0.1 M as a function of pH. The model outputs are in a good match with the experimental data. The higher pH in the system, the more negativity of zeta potential was developed at the oil-brine interface, which indicates more dissociated carboxylic acid groups $-COO^-$ are present in the aqueous solution as pH increases.

Kaolinite-brine Interface

To validate the model the measured zeta potential at the kaolinite-brine interface reported by Nasralla and Nasr-El-Din (2014) was replicated, as shown in to validate the model, as illustrated in Fig. 10. The concentrations of the electrolyte used in the experiment were 2, 10, and 50 g/l of NaCl [68]

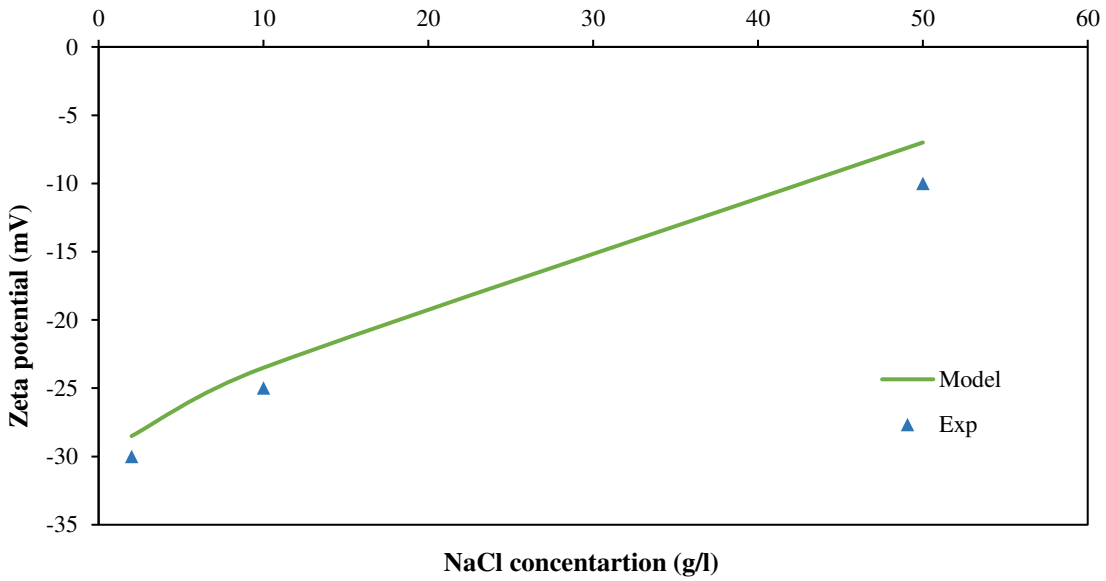

Fig. 10: Measured zeta potential at kaolinite-brine interface compared with the PHREEQC output.

The model outputs are in a good match with the measured data. However, a noticeable difference between the model and the measured value at NaCl concentration of 50 g/l was observed, which can be attributed to the limitation of Gouy-Chapman equation in predicting zeta potential at high electrolyte concentration wherein interactions between ions cannot be neglected [38].

In general, the differences between the model output and the measured data may arise from neglecting the mineral dissolution/precipitation reactions, and basal plane exchange reactions occur at the kaolinite surface. By considering the abovementioned reactions, the model performance can be further improved.

It is worth noting that zeta potential magnitude was calculated from the surface potential using Gouy-Chapman analytical solution, which is derived for a single symmetrical electrolyte such as NaCl which was used in this experiment. Therefore, the results were close to the measured values. However, the model output of zeta potential for mixed electrolyte (NaCl & CaCl2) is not expected to be as accurate as observed in the single electrolyte but still can serve as a valuable tool to predict the qualitative change in zeta potential trend and the subsequent wettability alteration. This limitation can be overcome by introducing a general solution for the Poisson-Boltzmann equation, as discussed in the recommendations.

B. Speciation in the COBR System

The speciation and surface charge development at the oil and rock surfaces owing to complex reactions occur COBR system was carried out in PHREEQC software by considering the injection of high salinity formation water that contains: 0.4 mol/l of NaCl and 0.005 mol/l of $CaCl_2$. The charge at the oil surface is developed by the contribution of the polarized carboxylic acid -COOH and nitrogen bases -NH exists at the oil-brine interface and the charge acquired by the interaction of calcium carboxylic acid -$COOCa^+$. Fig. 11 shows the concentration of the surface species developed at the oil-brine interface as a function of pH owing to the speciation in the COBR system at 100° C.

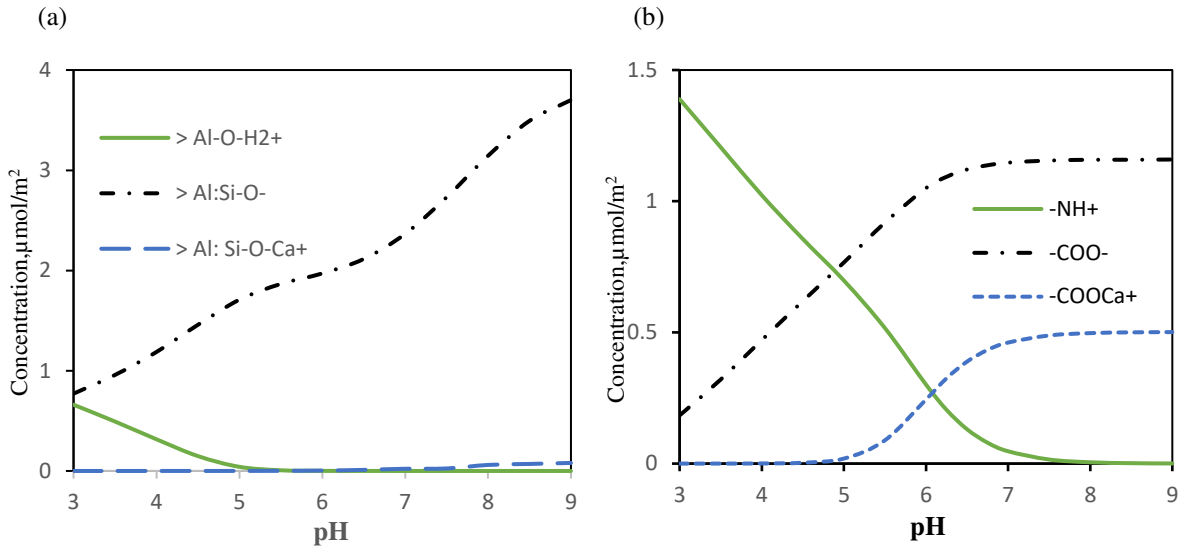

Fig. 11: Charged surface groups configuration developed at (a) the kaolinite surface (b) the oil surface.

Fig. 11 Shows the oil surface charge was dominated by the protonated nitrogen bases $-NH^+$ and then decreased sharply until pH 5, where the negatively charged carboxylic site took over and controlled the surface charge polarity. The dissociation of the carboxylic acid increase with pH until reaching some point where any further increase in the pH level has no longer effective in the dissociation reaction, and this is ascribed to the full ionization of the carboxylic acid. In this case, pH 7 is the maximum level above which no further $-COO^-$ is acquired at the oil surface. The contribution of calcium carboxylate surface species $-COOCa^+$ into the surface charge is less pronounced and influences the surface polarity above pH 5.

The surface charge at the kaolinite surface is developed by the protonation, deprotonation, and divalent cations sorption reactions that occur at the kaolinite surface. The pH-dependant speciation of the surface species at the kaolinite-brine interface is shown in Fig. 11, the kaolinite surface charge development is controlled by negatively charged surface species > Al: $Si\text{-}O^-$ which is the sum of > $Al\text{-}O^-$ and >$Si\text{-}O^-$, while the contribution of positively charged aluminol site > $Al\text{-}O\text{-}H_2^+$ is more pronounced at low pH levels but still does not dominate the surface polarity. The kaolinite sorbed calcium > Al: $Si\text{-}O\text{-}Ca^+$ starts to contribute to the rock surface charge at pH 8.

The surface functional groups at the kaolinite edge attract the oppositely charged species at the oil surface, forming the so-called electrostatic pair linkages, which represent the adhesive force between the two interfaces and are determined by multiplying the concentrations of the oppositely charged surface functional groups at both oil-brine and kaolinite brine interfaces.

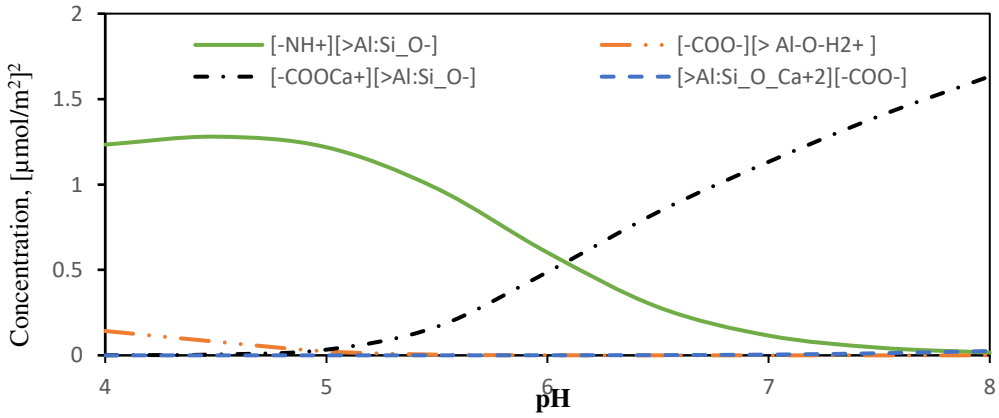

Fig. 12: Electrostatic pair linkages developed between the oil and kaolinite surfaces.

Fig. 12 depicts the electrostatic pair linkages developed between the oil and kaolinite surfaces at different pH levels. It can be observed that the adhesive force between the oil and kaolinite surfaces is created by the abundance

of the electrostatic bridges [-NH^+][> Al: Si-O^-] at pH less than five and the electrostatic pair linkage [-COOCa+][> Al: Si-O-] at pH higher than 5. Therefore, the composition of the injected water in the LSWF intercourse is manipulated to decrease the number of the electrostatic bridges, which leads to turns the wettability towards more water-wet and therefore, more oil can be desorbed from the kaolinite surface, and high oil recovery factor is obtained. It is worth noting that a low salinity effect can be observed even with low acid content in the oil, and this is primarily achieved by reducing the electrostatic bridge [-NH^+] [> Al: Si-O^-] at low pH levels, which elucidates the reason behind observing the low salinity effect at very low total acid number reported by Lager et al. (2008) [30]. The sum of the electrostatic pair linkages is termed Bond Product Sum (BPS), which is used to predict the wettability alteration in the COBR system owing to low salinity water flooding. The hypothesis is that low salinity injected-brine should reduce the adhesive forces between the oil and rock surfaces, hence decreasing the BPS. However, this approach is not applicable at a pH level higher than 5.

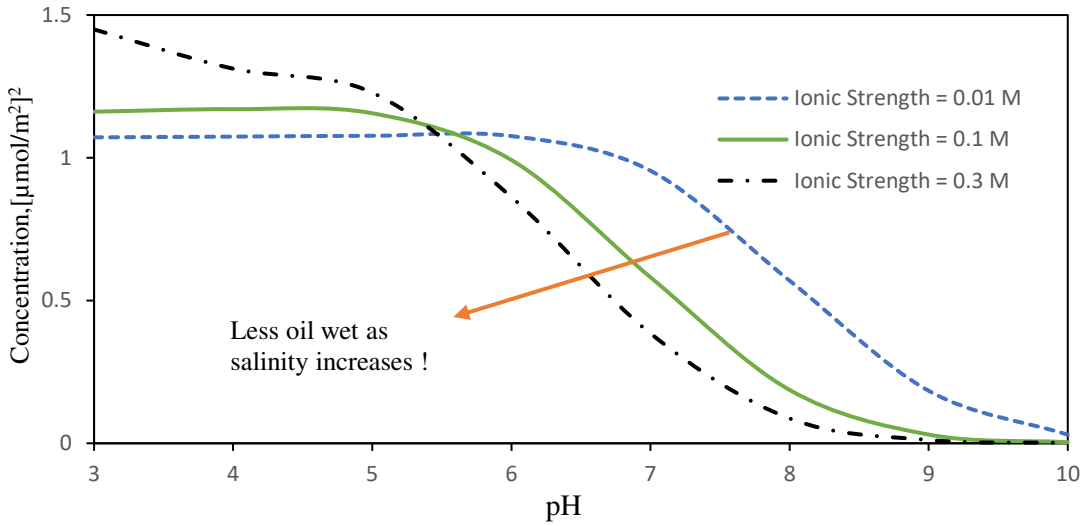

Fig. 13: The bond product sum prediction under the effect of different ionic strengths of injected brine.

Fig 13 shows the BPS's determination for aqueous solutions at different ionic strengths, which implies different salinities, the concentration of NaCl in the aqueous solutions was 0.4, 0.1, and 0.01 mole/l. It can be observed that lowering the injected brine salinity results in a lower BPS for pH values less than five, which in turn lead to more water-wet condition and higher oil recovery. In contrast, the BPS values increased by decreasing the injected-water salinity for pH levels higher than five, meaning that rock wetness becomes more oil-wet, which contradicts the theory behind the low salinity effect. Therefore, the BPS method can predict the LSE only at low pH levels. For higher pH values, zeta potential and stability number approaches can be used to observe the LSE.

C. Effect of the pH Level

The pH of the aqueous solution is a measure of the hydrogen ions concentration in the system. The higher the hydrogen ions concentration, the lower the pH is. The pH level controls the acid/base reactions in the COBR system, which affects the solid-aqueous speciation and the surface charge development at the interfaces of the oil-brine and kaolinite-brine wettability of the system.

To address the effect of the pH on oil recovery, brine with an ionic concentration of 0.056 M was injected into a high salinity formation water,with the ionic strength of 0.23 M, at different pH levels, the developed zeta potentials at both oil and kaolinite surfaces are shown in Fig. 14.

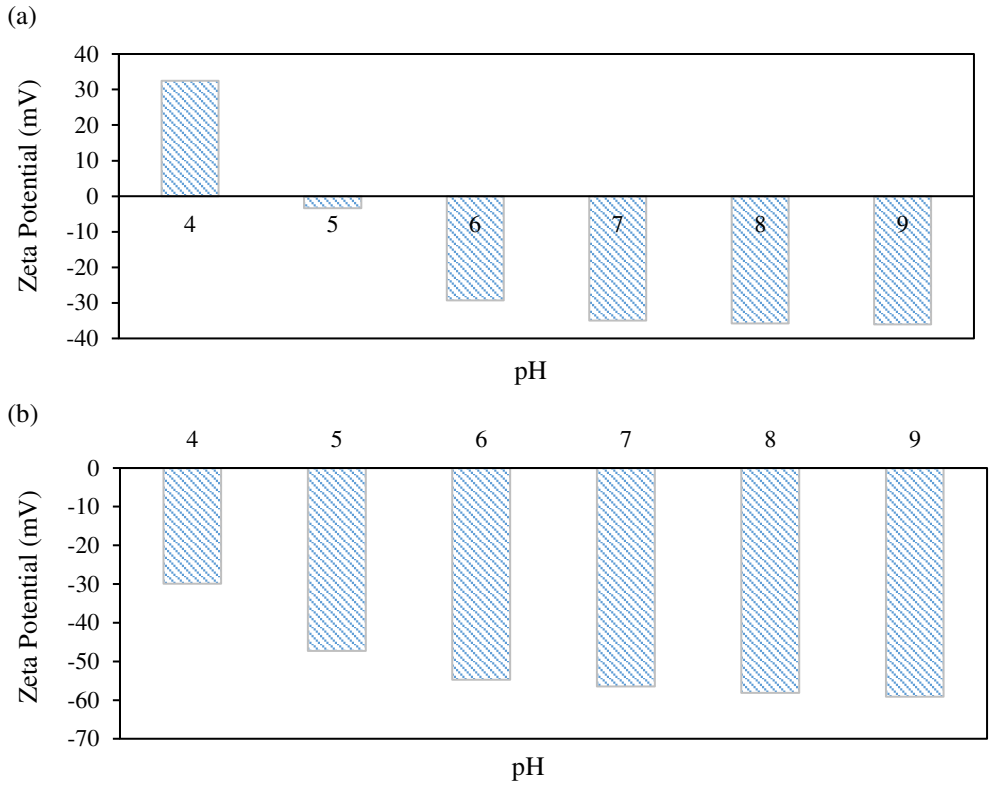

Fig. 14: Zeta potential development under the effect of pH, (a) oil surface (b) kaolinite surface.

The negativity of zeta potential at the kaolinite-brine interface increases with pH owing to more deprotonation of aluminium and silica edge sites Al: Si-OH at high levels of pH. A similar trend of zeta potential is observed at the oil-brine interface for a pH greater than 4, owing to more dissociation of the carboxylic acid group -COOH. However, no further increase in zeta potential was noticed above pH eight at the oil-brine and kaolinite-brine interfaces and this ascribed to the full ionization of the abovementioned surface functional groups, which in turn prevent acquiring more negative charges at the oil and rock surfaces. The higher negativity of zeta potential at the oil-brine and kaolinite-brine interfaces result in more electrostatic repulsive forces between the two interfaces, meaning that more stabilization of the thin water film spread on the rock surface and the expansion of the electrical double-layer thickness is established, and therefore wettability alteration towards more water-wet is induced, and more oil is recovered. For pH 4, the polarity of zeta potential at the oil-brine interface is positive due to the higher concentration of the protonated nitrogen bases $-NH^{+}$ compared to dissociated carboxylate group -COO-. Hence, the electrostatic attraction forces between the oil-brine and kaolinite-brine interfaces are developed, leading to rupturing the water layer between the two interfaces, turning the rock surface to more oil-wet, and less amount of oil is recovered. So the higher the pH level, the more negative the surface charge developed at the oil and rock surfaces, the stronger the electrostatic repulsive forces are created, and the rock becomes more water-wet, resulting in higher oil recovery. These results are in line with experimental measurements performed on Berea sandstone rocks wherein the decrease in zeta potential magnitude from -22 mV to -10 and from -15 to -8 at the interfaces of oil-brine and rock-brine was observed by lowering the pH of the system from 7.3 to 4.8. They confirmed their results by measuring the contact angles at the specified pH levels. They also stated that the increase in oil recovery due to the pH rise during LSWF could be accomplished by either expanding the EDL or decreasing the interfacial tension between the oil and water. [20].

D. Effect of the Ionic Strength

To address the effect of the ionic strength on the oil recovery owing to LSE; high salinity formation water with ionic strength of 0.23 M was diluted by reducing the concentration of the monovalent and divalent ions, which results in aqueous solutions with ionic strength of 0.115 M and 0.056 M. The formation-brine and the diluted

aqueous solutions were separately flooded into a hydrocarbon system, and the developed zeta potentials at both oil-brine and kaolinite-brine interfaces is shown in Fig. 15 as a function of pH.

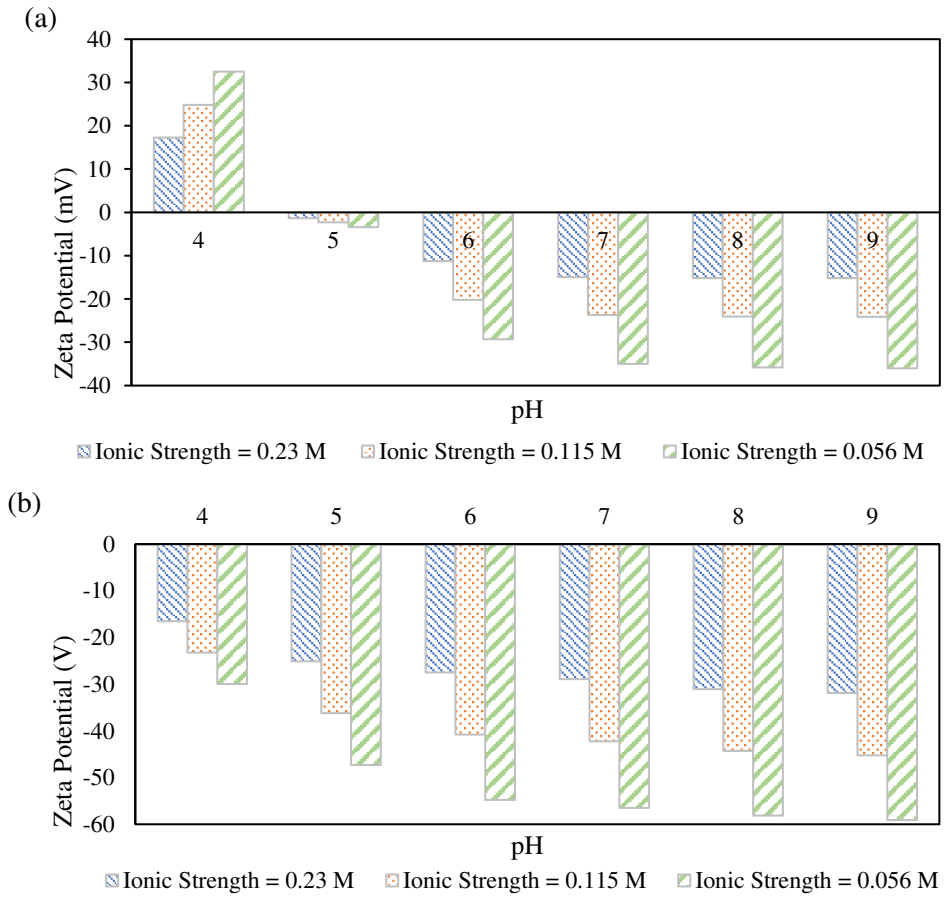

Fig. 15: Zeta potential development under the effect of ionic strength at, (a) oil-brine interface (b) kaolinite-brine interface.

Considering the surface charge development at the kaolinite-brine interface, the negativity of zeta potential is continuously increasing as pH rise due to higher dissociation of kaolinite surface species at higher pH levels. By considering the charge development at pH 6, the ionic strength of 0.23 M (conventional waterflooding) results in zeta potential of -29 mV. This magnitude is increased to -40 mV by lowering the ionic strength to 0.115 M, whereas the further increase in zeta potential to -55 mV was observed when the ionic strength was reduced to 0.056 M, this increase in potential is ascribed to the lower abundance of the counterions exist at the electrical interfacial region caused by lowering the ionic strength of injected brine which in turns decrease the ability to screen off the negative charges at the kaolinite surface and therefore higher negative potential at the slip plane was developed, the same trend of zeta potential with different ionic strength was observed at a given range of pH.

For the surface charge development at the oil-brine interface at pH 6, zeta potential increased from -11 mV in the conventional waterflooding to – 20 mV, where the ionic strength is reduced to 0.115 M while the further increase was obtained by lowering the ionic strength to 0.056 M wherein the potential reached -29 mV. The increase in the potential at the oil surface acquired by lowering the ionic strength is attributed to the decrease in the abundance of the surface functional group -NH+ at low pH, and the decrease of the surface species -$COOCa^{+}$ at high pH levels.

Lowering the ionic strength increases both the thickness of the EDL and the negative polarity at the oil-brine and kaolinite-brine interfaces, resulting in stronger electrostatic repulsive forces between the two interfaces, which stabilizes the water film spread on the surface rock, allowing more oil to be recovered. However, reducing the ionic strength may increase the positive zeta potential magnitude as observed at pH 4, which increases the attraction forces between the oil surface and negatively charged kaolinite surface. As a result, wettability towards more oil-wet is obtained and this may elucidate why LSE failed to observe in some cases.

The pH required to dissociate the carboxylic acid -COOH entirely also depends on the ionic strength. The higher the ionic strength, the more pH value is needed to obtain a full ionization of -COOH. For instance, zeta potential magnitude continuous to increase until pH 9 for the highest ionic strength (0.23 M) while the increase is suppressed at pH 7 for the lowest ionic strength (0.056 M), which implies the full ionization of the surface group -COOH at that level of pH.

These results are consistent with observations highlighted by Jackson et al. (2018), who performed a core flood experiment on sandstone rocks wherein the higher negativity of zeta potential is obtained when the ionic strength was reduced from 2 M to 0.015 M in the presence and absence of the divalent ions [69].

E. Effect of the Divalent Cation in the Injected-brine

Fig. 16 shows zeta potential development at both oil-brine and kaolinite-brine interfaces as a function in pH a. In general, the negativity of zeta potential increases with pH rise regardless of the injected-brine composition.

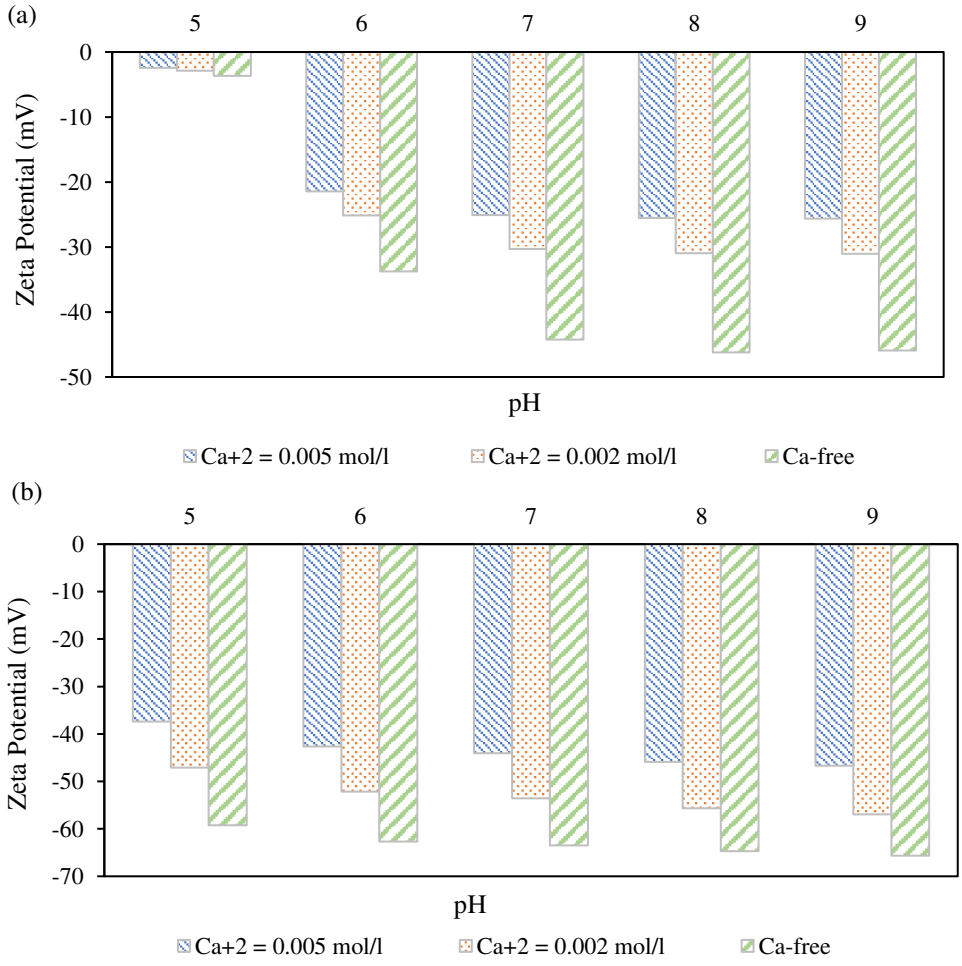

Fig. 16: Zeta potential development under the effect of divalent cation concentration in the injected brine, (a) oil-brine interface (b) kaolinite-brine interface.

By considering the surface charge development at pH 6, zeta potential magnitude becomes more negative with lower calcium ions concentration. For instance, the potential at the interfaces of the oil-brine and kaolinite-brine was -22 and -42 mV, respectively, when the concentration of Ca^{+2} is 0.005 mol/l. However, the potential became more negative when the Ca-level was reduced to 0.002 mol/l, e.g., -25 and -52 mV at the oil and kaolinite surfaces, respectively, the highest increase in zeta potential -34, -62 mV was acquired by totally removing the Ca+2 from the injected brine, the lower Ca^{+2} results in a lower concentration of positively charged surface groups $-COOCa^{+}$, >Al: Si-O-Ca^{+} at the oil and rock surfaces, which lead to increase the potential at the slip plane (zeta potential), and therefore the more electrostatic repulsive force is induced between the interfaces of the oil-brine and kaolinite-brine and, as a result, more stability of the water film spread on the rock surface is established, meaning that the

rock wetness turns further water wet and high oil recovery is obtained. Furthermore, the absence of the calcium ions in the injected brine leads to a decrease in the number of developed bridges between the dissociated oil species and negatively charged kaolinite surface, which in turn results in further oil desorption. The results were emphasised by calculating the stability number at pH six as a function of divalent cation concentration, as shown in Fig. 17.

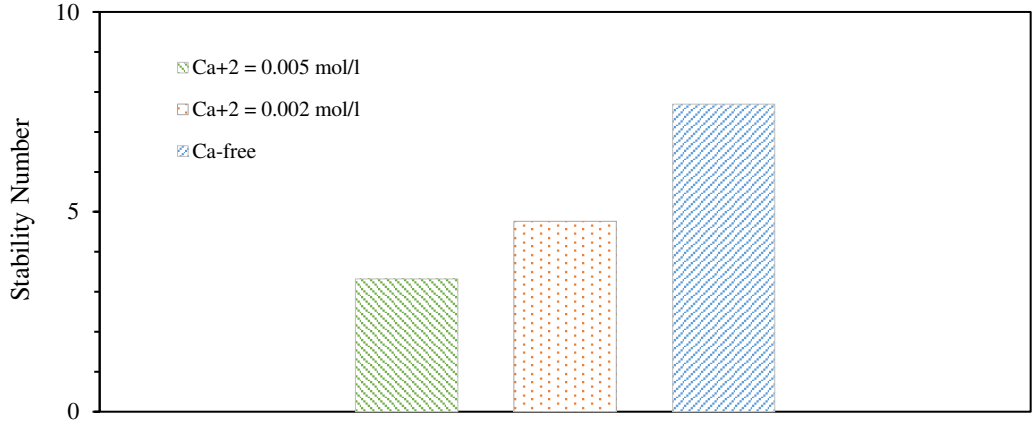

Fig. 17: Stability number under the effect of the divalent cation concentration at pH 6.

It can be observed that the stability number was greater than one at all brine compositions, which implies the domination of the electrostatic repulsive forces over Van der Waals attraction forces. The stability number increased from 3.5 to 5 by lowering Ca^{+2} concentration from 0.005 to 0.02 mol/l, and the further increase (SN = 8.5) was achieved when the Calcium-free brine composition was injected, meaning that higher oil recovery could be obtained.

These results are consistent with the findings reported by Nasralla and Nasr-El-Din (2014) conducted a core flood experiment on Berea sandstone rocks wherein the oil recovery was significantly increased by injecting brine containing 200 ppm of NaCl in comparison with the same brine concentration of CaCl2 [68].

F. Effect of Divalent Cations in the Formation water

To address the effect of the divalent cation concentration/ type in the formation water; low salinity brine is injected into three different water compositions, Fw_1, Fw_2, and Fw_3, the calcium ions concentration in Fw_1 is 0.005 mol/l and reduced to 0.002 mol/l in Fw_2, Fw_3 is the same as Fw_2, but the Ca^{+2} ions were replaced by Mg^{+2} while the ionic strength is kept constant at the three formation water compositions as illustrated in Table 4.

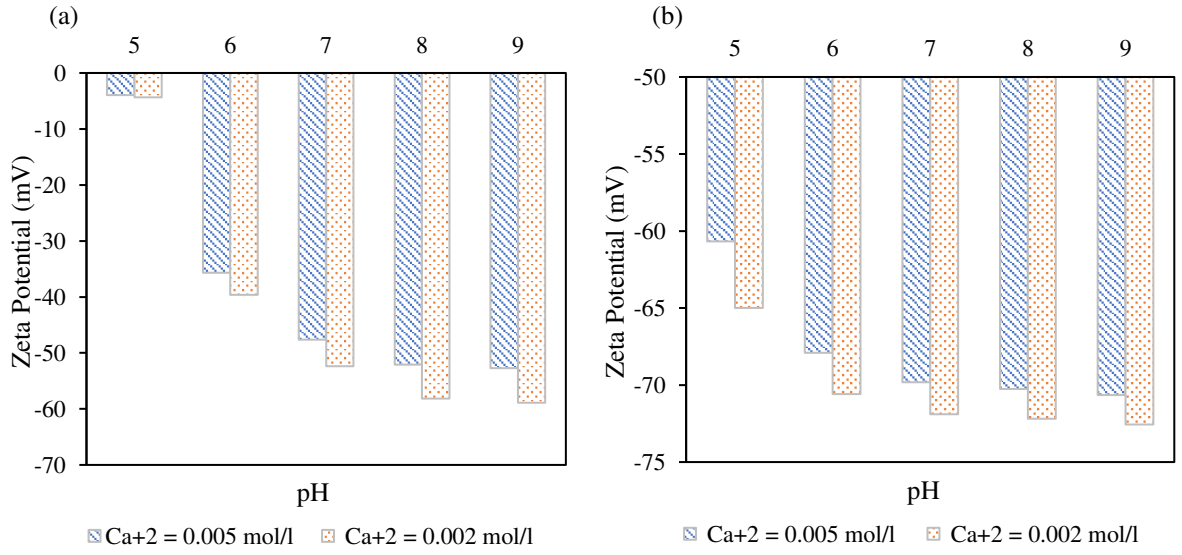

Fig. 18: Zeta potential development under the effect of divalent cation concentration in the formation water, (a) oil-brine interface (b) kaolinite-brine interface.

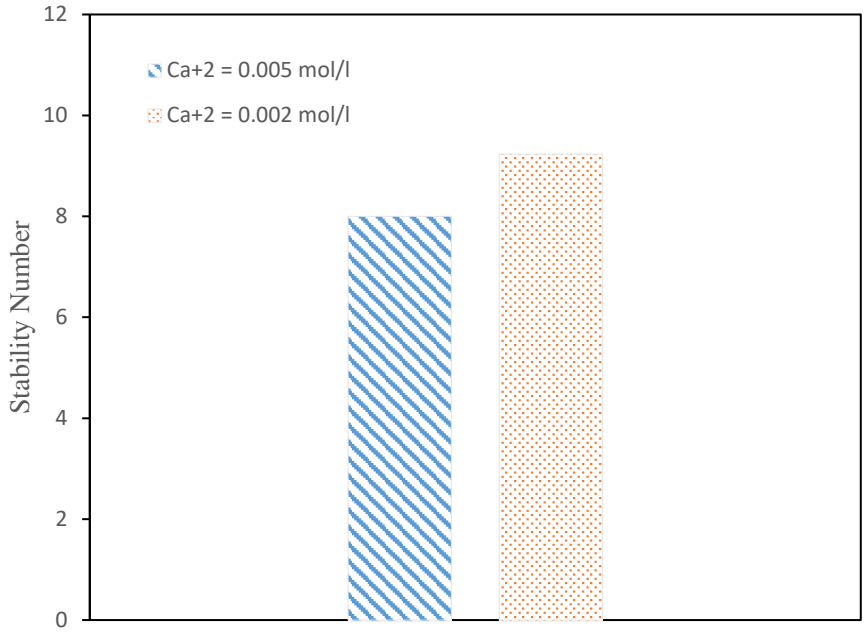

Fig. 19: stability number under the effect of divalent cation concentration in the formation water.

Fig. 18 shows zeta potential development at both oil-brine and kaolinite-brine interfaces as a function of pH. In general, the negativity of zeta potential increases with pH rise regardless of the formation water composition. By considering the surface charge development under the effect of the divalent cation concentration in the formation water at pH 6, reducing the Ca^{+2} from 0.005 to 0.002 mol/l caused a slight increase in zeta potential magnitude from -37 to -40 and from -71 to -72 mV at the oil-brine and kaolinite-brine interfaces, respectively, which lead to increase the repulsive force between the two interfaces, and therefore wettability alteration towards more water-wet is induced. The same feature was captured by the stability number approach as shown in Fig. 19, where the higher repulsive force owing to lower Ca^{+2} concentration increased the stability number, and therefore the more stable condition of the water film spread on the surface rock was established in Fw_2, and the rock turns further water-wet.

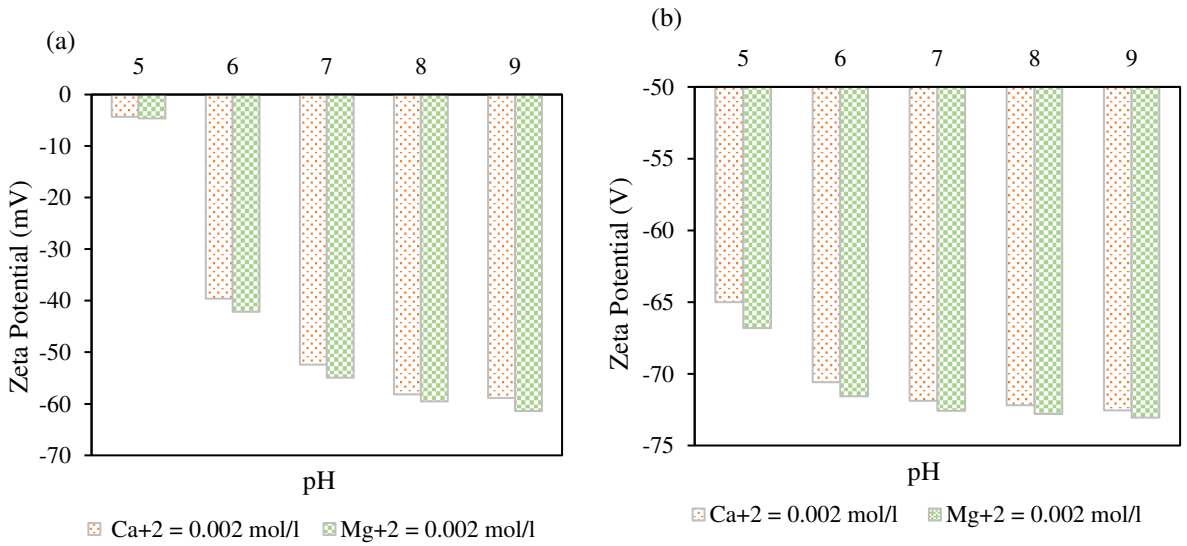

Fig. 20: Zeta potential development under the effect of divalent cation type, (a) oil-brine interface (b) kaolinite-brine interface.

The effect of the divalent cation type in the formation water is demonstrated in Fig. 20, wherein the negative zeta potential value increased by the replacement of Ca^{+2} by Mg^{2} at pH 6. For instance, zeta potential at the oil and

kaolinite surfaces was -40 and -72 mV, respectively, in the presence of calcium ions. However, the potential became more negative when Ca^{+2} was totally replaced by magnesium ions in the formation water, e.g., -42 and -73 mV was developed at the oil and kaolinite surfaces, respectively, which in turn led to developing higher repulsive forces between the two surfaces, meaning that the rock turns more water-wet, and higher oil is recovered. The stability number was higher in the presence of Mg^{+2} compared with Ca^{+2} (refer to Fig. 21), which emphasizes the stabilization of the thin water layer spread on the surface rock and higher oil desorption in the case of Mg^{+2}.

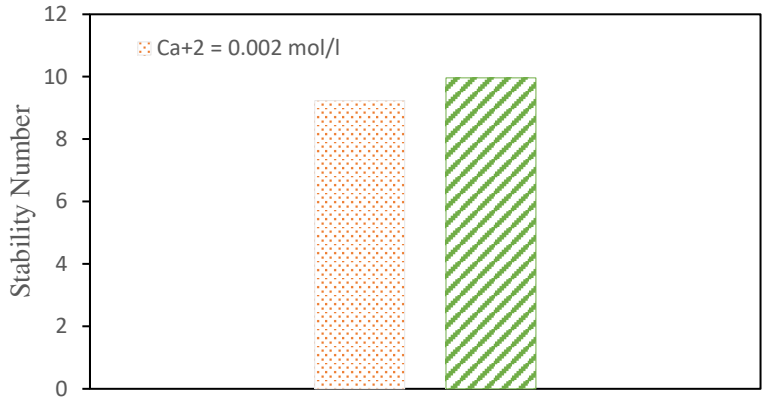

Fig. 21: stability number under the effect of divalent cation concentration in the formation water.

The higher potential magnitude owing to lower Ca^{+2} concentration in the formation water is primarily caused by minimizing the number of the surface species -$COOCa^{+}$ developed at the oil-brine interface, as shown in Fig. 22. The same concentration of Ca^{+2} and Mg^{+2} in the formation water results in creating a greater number of surface species of $COOCa^{+}$ than $COOMg^{+}$ as shown in Fig. 23, as the results more negative charge is developed at the oil surface in the presence of Mg^{+2}, which elucidates why zeta potential is higher in the case of Mg^{+2}.

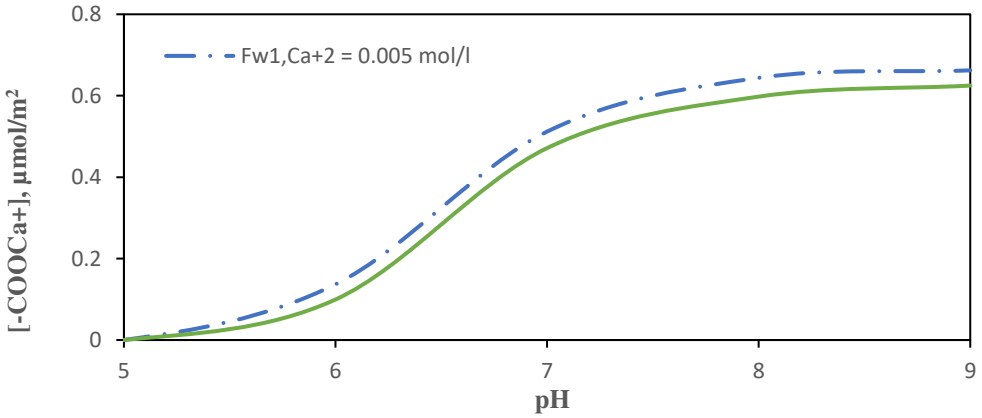

Fig. 22: Calcium carboxylate concentration at the oil surface under the effect of different Ca^{+2} level.

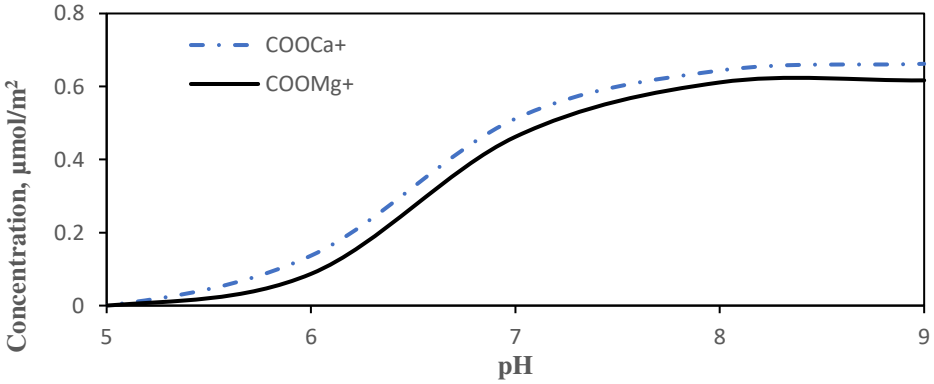

Fig. 23: Divalent cation sorbed affinity at the oil surface under the effect of divalent ions type.

These results are in line with the experimental measurements reported by Al-Saedi et al. (2019), who conducted a series of core floods on Berea sandstone rocks at reservoir temperature 90 °C wherein the incremental oil recovery was increased by 4 % when the concentration of the calcium ions in the formation brine was reduced to the half in a tertiary mood of low salinity waterflooding process. It was also observed that the incremental oil recovery jumped from 5% to 17.5 % when Ca^{+2} was equally replaced by Mg^{+2} in the formation water [70].

G. Oil composition

The surface charge development at the oil-brine interface is controlled by the total amount of oil active species that exist at the interface, which is usually represented by the amount of acid and base compounds traveled into the oil-brine interface. The deprotonated carboxylic acid, divalent cation sorbed, and to a less extent, the protonated nitrogen bases have controlled the polarity of the oil-brine interface [21]. The number of site density of oil surface species available for hydrogen exchange (protonation and deprotonation) is linearly correlated to the total acid number (TAN) and the total base number (TBN), which are affected by the oil composition [21]. The effect of the oil composition on the surface charge development at both oil-brine and kaolinite-brine interfaces and the subsequent wettability alteration is examined by determining zeta potential magnitudes at the two interfaces at different acid/base ratios of crude oil emulsion as a function of pH, as shown in Fig 24.

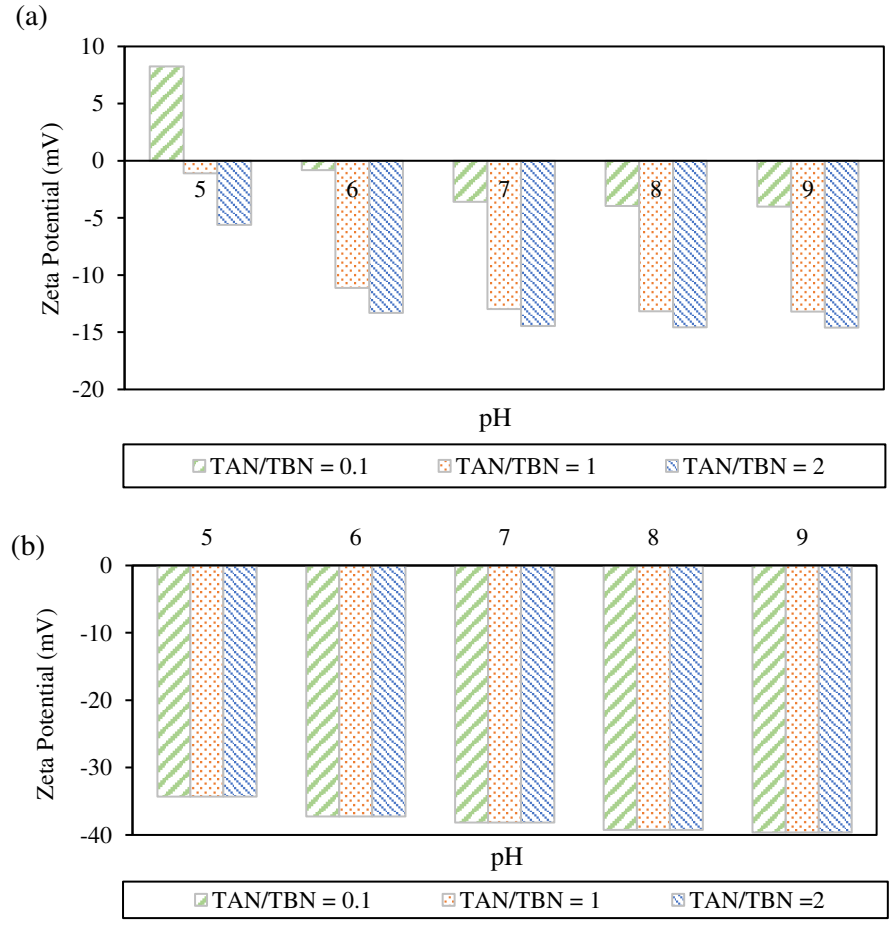

Fig. 24: Zeta potential at different acid/base ratio, (a) oil-brine interface (b) kaolinite-brine interface.

According to Fig. 24, the calculated zeta potential magnitudes at the kaolinite-brine interface showed a negative polarity ranging from -33 to -40 mV, depending on the pH level. However, the acid/base ratio has no effect on the developed zeta potential at a specified pH level. In contrast, varying the crude oil acid/base ratio, which implies the change in the total acid number, profoundly impacts the speciation and surface charge development at the oil-brine interface. For instance, for pH values greater than 6, zeta potential has a negative polarity that increases by increasing the acid/base ratio, and this is ascribed to the increase in the abundance of negatively charged surface groups (-COO-) owing to more dissociation of the carboxylic acid. The higher negativity of zeta potential in the

oil-brine interface results in greater electrostatic repulsive force between the oil-brine and kaolinite-brine interfaces, which leads to more water wetness and more oil droplets from the oil-brine the kaolinite surface is desorbed. For pH 4, zeta potential has a positive polarity for the three total acid numbers. The higher the acid/base ratio, the less positive zeta potential is. Thereby lower attraction force is developed between the oil-brine and the kaolinite-brine interfaces, which results in a less oil-wet condition. Moving to pH 5, the lower acid/base ratio 0.1 results in developing a positive polarity at the oil-brine interface due to the domination of the positive surface species created by the protonation of the basic nitrogen compounds (-NH+); as a result, the attraction force is induced between the opposite polarity of the oil-brine and kaolinite-brine interfaces, leading to more oil adhesion into the rock surface and less water-wet condition. While the higher degree of oil desorption is acquired by the increase of the acid/base ratio to 1 and further water-wet condition, and more oil desorption is achieved at the highest acid/base ratio 2. The combination of pH and total acid/base contents in the crude oil emulsion control the polarity at the oil-brine interface that determines the electrostatic forces between the oil-brine and the kaolinite-brine interfaces which in turn control the stability of the water film spread on the rock surface and the subsequent wettability alteration.

Prediction of wettability alteration using the stability number approach is more comprehensive than the zeta potential method. The latter only considers the attraction/repulsion forces developed between the oil-brine and the kaolinite-brine interfaces owing to the electrostatic forces to express the change in the double layer thickness and the subsequent wettability alteration, while the former involves both the electrostatic forces and Van der Waals forces to calculate the net forces created between the two interfaces and then predict the stability of the thin water film spread on the rock surface and the related wettability change. Therefore, the wettability alteration is also examined by calculating the stability number of the crude oil emulsion at different acid/base ratios as a function of pH, as shown in Fig. 25.

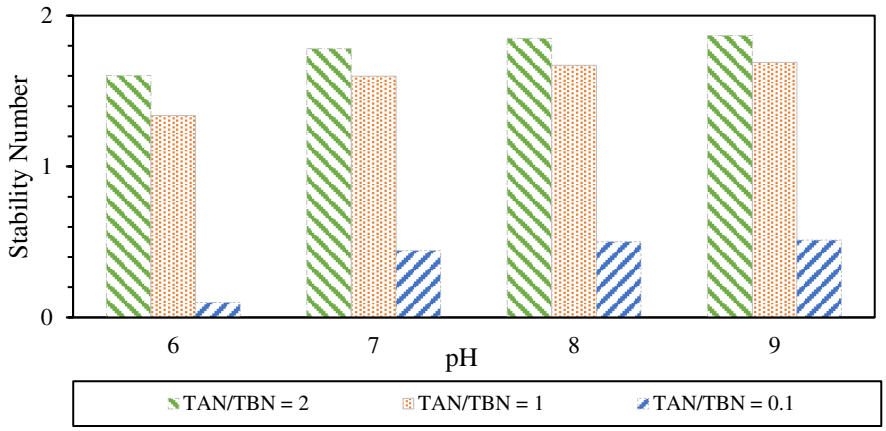

Fig. 25: Stability number of crude oil emulsions with different acid/base ratios.

It can be observed that the stability number for the lowest acid/base ratio (TAN/TBN= 0.1) was less than one for a given range of pH, which indicates the domination of the Van der Waals attraction forces between the oil-brine and kaolinite-brine interfaces which lead to rupture the thin water film spreads on the mineral surface and therefore the more oil-wet condition is encountered, and less amount of oil droplets can be released from the rock surface. Increasing the acid/base ratio results in stability number values greater than one, which implies the domination of the electrostatic repulsive forces wherein the wettability alteration towards more water-wet conditions is achieved. Therefore, more oil droplets are released from the kaolinite surface. At a given pH level, the higher the acid/base ratio in the crude oil emulsion, the higher the stability number is achieved. However, the increase in stability number due to pH rise is relatively small as moving towards high pH levels, which is attributed to the decrease in the rate at which the carboxylic acid is dissociated.

It is worth noting that, at pH greater than 6, the crude oil emulsion with an acid/base ratio of 0.1 revealed repulsive electrostatic forces between the oil-brine and the kaolinite-brine interfaces, which indicates the prevailing of the water-wet condition in the system. However, the oil-wet condition is predicted using the stability number approach wherein the effect of Van der Waals attraction force is incorporated. Therefore, it can be argued that using the electrostatic forces as a determinant factor for the wettability alteration without considering Van der Waals attraction force might be misleading. These outcomes are in line with the results achieved by Takeya et al. (2019),

who developed a triple-layer surface complexation model wherein zeta potential at the crude oil emulsion is increased by the increase of the acid/base content [19]. Furthermore, Bonto et al. (2019), who developed a diffuse layer surface complexation model, reached a similar result of increasing the negative zeta potential value at a higher accumulation of acid compounds at the oil-brine interface [21].

5. Conclusion

Low salinity waterflooding induces the wettability alteration towards a more water-wet condition in the COBR system due to the stabilization of the thin water film that exists between the oil-brine and rock-brine interfaces. The wettability modification and the related degree of oil desorption are controlled by different factors such as ionic strength, divalent cations type/concentration, oil composition, and pH levels in the system.

- The higher the pH level in the system, the more negative surface charge developed at oil-brine and rock-brine interfaces. Therefore, higher electrostatic repulsive forces are created, leading to more water-wet conditions. However, above a certain pH level, no further oil desorption can be acquired due to the complete ionization of the surface species accumulated at both oil and rock surfaces.
- Decreasing the ionic strength of the injected brine reduces the abundance of the counterions in the interfacial electrical region, which in turn leads to expanding the double layer. Therefore, wettability turns towards more water-wet, and more oil is recovered.
- Decreasing the Ca^{+2} concentration in the injected brine lowers the abundance of both surface functional groups -$COOCa^{+}$ and >Al: Si-O-Ca^{+} at the oil and kaolinite surfaces, respectively, resulting in more repulsive forces and less oil affinity to the kaolinite surface, meaning that the rock will be more water-wet and more oil can be recovered.
- Decreasing the Ca^{+2} concentration in the formation water results in developing more negative charges at both oil and rock surfaces due to lower concentration of the surface groups -$COOCa^{+}$ and >Al: Si-O-Ca^{+} at the oil and kaolinite surfaces, respectively, which increases the electrostatic repulsion forces between the oil-brine and kaolinite-brine interfaces and therefore, the rock turns towards more water-wet which in turns lead to more oil desorption and higher oil recovery. Replacing the calcium ions Ca^{+2} by magnesium ions Mg^{+2} in the formation water results in more negative charges at the oil-brine and kaolinite-brine interfaces, meaning that higher oil recovery can be obtained.
- The more acidic compounds in the oil composition, the more dissociated carboxylic acid -COO- and greater electrostatic repulsive forces between the oil and kaolinite surfaces are developed. Hence, more oil desorption from the rock surface is established.

Oil composition with rich base contents can exhibit positive surface charges at low pH levels. Therefore, increasing the negativity of zeta potential at the rock surface due to low salinity waterflooding increases the attraction forces between the oil and rock surfaces. Meaning that less water-wet is established, which can elucidate the failure in observing low salinity effect in some cases

The surface complexation-based model can be further developed by introducing the mineral equilibrium phases reactions, multi ion-exchange reactions that occur at the basal plane of the kaolinite surface, and the effect of the soluble carbon dioxide in the oil. The effect of the CO_2 injection can also be incorporated into the code as a new feature that significantly affects the pH level in the crude oil/brine/rock system.

Gouy-Chapman analytical solution is derived based on (1:1) electrolyte such as (NaCl), which leads to error in zeta potential calculation. However, this issue can be overcome by following the procedure introduced by Brokvec and Westal, who proposed a useful analytical solution for the Poisson Boltzmann equation accounted for mixed electrolyte (NaCl & $CaCl_2$) [19].

The more accurate prediction of zeta potential can be determined using a triple-layer surface complexation model wherein more details of the interfacial electrical layer are incorporated. However, more parameters are required to be set.

Declarations

- **Availability of data and materials**
  All data and accompanying analysis code are available from the author on reasonable request.

- **Competing interests**
  The authors declare that they have no competing interests.

- **Funding**
  This work was financially supported by the ministry of higher education in Sudan.

- **Author contributions**
  Oubai Elagab has numerically investigated the effects of oil acid/base number, system pH level, and divalent cations concentration in the injected water on improving oil recovery during low salinity waterflooding in sandstone reservoirs. by developing a surface complexation based-model accounting for double layer expansion in the interfacial region at the kaolinite-brine and oil-brine interfaces using a geochemical reaction path code PHREEQC, where complex chemical reactions in the crude oil, brine, rock system (COBR) are captured.

Acknowledgments
I would like to thank all my instructors for their immense academic impact and support.

References

[1] Exxon Mobil Corporation, (2017). *2018 Outlook for Energy: A View to 2040,* Available at: https://corporate.exxonmobil.com/en/~/media/Global/Files/outlook-for-energy/2018-Outlook-for-Energy.pdf
[2] Toews, G. and Naumov, A., (2015). The relationship between oil price and costs in the oil industry, *The Energy Journal,* **36** pp.237-254.
[3] Ahmed, T., (2018). Reservoir Engineering Handbook. Gulf Professional Publishing.
[4] Craig, F.F., (1971). The Reservoir Engineering Aspects of Waterflooding. HL Doherty Memorial Fund of AIME New York.
[5] Winoto, W., Loahardjo, N., Xie, S.X., Yin, P. and Morrow, N.R., (2012). Secondary and tertiary recovery of crude oil from outcrop and reservoir rocks by low salinity waterflooding, *SPE Improved Oil Recovery Symposium,*
[6] Sheng, J., (2014). Critical review of low-salinity waterflooding, *Journal of Petroleum Science and Engineering,* **120** pp.216-224.
[7] RezaeiDoust, A., Puntervold, T., Strand, S. and Austad, T., (2009). Smart water as wettability modifier in carbonate and sandstone: A discussion of similarities/differences in the chemical mechanisms, *Energy & Fuels,* **23** (9), pp.4479-4485.
[8] Jackson, M., Vinogradov, J., Hamon, G. and Chamerois, M., (2016). Evidence, mechanisms and improved understanding of controlled salinity waterflooding part 1: Sandstones, *Fuel,* **185** pp.772-793.
[9] Al Shalabi, E.W. and Sepehrnoori, K., (2017). Low Salinity and Engineered Water Injection for Sandstone and Carbonate Reservoirs. Gulf Professional Publishing.
[10] Xie, Q., Liu, Y., Wu, J. and Liu, Q., (2014). Ions tuning water flooding experiments and interpretation by thermodynamics of wettability, *Journal of Petroleum Science and Engineering,* **124** pp.350-358.
[11] McGuire, P., Chatham, J., Paskvan, F., Sommer, D. and Carini, F., (2005). Low salinity oil recovery: An exciting opportunity for alaska's north slope, *SPE 93903 Presented at the Western Regional Meeting Held in Irvin, CA,*
[12] Austad, T., RezaeiDoust, A. and Puntervold, T., (2010). Chemical mechanism of low salinity water flooding in sandstone reservoirs, *SPE Improved Oil Recovery Symposium,*
[13] Aladasani, A., Bai, B., Wu, Y. and Salehi, S., (2014). Studying low-salinity waterflooding recovery effects in sandstone reservoirs, *Journal of Petroleum Science and Engineering,* **120** pp.39-51.
[14] Al-Saedi, H.N. and Flori, R.E., (2018). Enhanced oil recovery of low salinity water flooding in sandstone and the role of clay, *Petroleum Exploration and Development,* **45** (5), pp.927-931.
[15] Brady, P.V., Morrow, N.R., Fogden, A., Deniz, V. and Loahardjo, N., (2015). Electrostatics and the low salinity effect in sandstone reservoirs, *Energy & Fuels,* **29** (2), pp.666-677.
[16] Buckley, J., Liu, Y. and Monsterleet, S., (1998). Mechanisms of wetting alteration by crude oils, *SPE Journal,* **3** (01), pp.54-61.

[17] Jerauld, G.R., Lin, C.Y., Webb, K.J. and Seccombe, J.C., (2008). Modeling low-salinity waterflooding, *SPE Reservoir Evaluation and Engineering,* **11** (6), pp.1000-1012.
[18] Pouryousefy, E., Xie, Q. and Saeedi, A., (2016). Effect of multi-component ions exchange on low salinity EOR: Coupled geochemical simulation study, *Petroleum,* **2** (3), pp.215-224.
[19] Takeya, M., Shimokawara, M., Elakneswaran, Y., Okano, H. and Nawa, T., (2019). Effect of Acid Number on the Electrokinetic Properties of Crude Oil during Low-Salinity Waterflooding, *Energy & Fuels,* **33** (5), pp.4211-4218.
[20] Nasralla, R.A. and Nasr-El-Din, H.A., (2014). Double-layer expansion: is it a primary mechanism of improved oil recovery by low-salinity waterflooding? *SPE Reservoir Evaluation & Engineering,* **17** (01), pp.49-59.
[21] Bonto, M., Eftekhari, A.A. and Nick, H.M., (2019). An overview of the oil-brine interfacial behavior and a new surface complexation model, *Scientific Reports,* **9** (1), pp.6072.
[22] Ligthelm, D.J., Gronsveld, J., Hofman, J., Brussee, N., Marcelis, F. and van der Linde, H., (2009). Novel waterflooding strategy by manipulation of injection brine composition. *EUROPEC/EAGE Conference and Exhibition,*
[23] Jadhunandan, P. and Morrow, N., (1991). Spontaneous imbibition of water by crude oil/brine/rock systems, *In Situ;(United States),* **15** (4),
[24] Tang, G. and Morrow, N.R., (1997). Salinity, temperature, oil composition, and oil recovery by waterflooding, *SPE Reservoir Engineering,* **12** (04), pp.269-276.
[25] Yildiz, H.O. and Morrow, N.R., (1996). Effect of brine composition on recovery of Moutray crude oil by waterflooding, *Journal of Petroleum Science and Engineering,* **14** (3-4), pp.159-168.
[26] Webb, K., Black, C. and Al-Ajeel, H., (2003). Low salinity oil recovery-log-inject-log, *Middle East Oil Show,*
[27] Webb, K., Black, C. and Edmonds, I., (2005). Low salinity oil recovery–The role of reservoir condition corefloods, *IOR 2005-13th European Symposium on Improved Oil Recovery,*
[28] Tang, G. and Morrow, N.R., (1999). Influence of brine composition and fines migration on crude oil/brine/rock interactions and oil recovery, *Journal of Petroleum Science and Engineering,* **24** (2-4), pp.99-111.
[29] Cissokho, M., Bertin, H., Boussour, S., Cordier, P. and Hamon, G., (2010). Low salinity oil recovery on clayey sandstone: Experimental study, *Petrophysics,* **51** (05),
[30] Lager, A., Webb, K.J., Black, C., Singleton, M. and Sorbie, K.S., (2008). Low salinity oil recovery-an experimental investigation1, *Petrophysics,* **49** (01),
[31] Johnston, N. and Beeson, C.M., (1945). Water permeability of reservoir sands, *Transactions of the AIME,* **160** (01), pp.43-55.
[32] Bernard, G.G., (1967). Effect of floodwater salinity on recovery of oil from cores containing clays, *SPE California Regional Meeting,*
[33] Alagic, E. and Skauge, A., (2010). Combined low salinity brine injection and surfactant flooding in mixed−wet sandstone cores, *Energy & Fuels,* **24** (6), pp.3551-3559.
[34] Jackson, M.D., Al-Mahrouqi, D. and Vinogradov, J., (2016). Zeta potential in oil-water-carbonate systems and its impact on oil recovery during controlled salinity water-flooding, *Scientific Reports,* **6** pp.37363.
[35] Zhang, Y. and Morrow, N.R., (2006). Comparison of secondary and tertiary recovery with change in injection brine composition for crude-oil/sandstone combinations, *SPE/DOE Symposium on Improved Oil Recovery,*
[36] Valocchi, A.J., Street, R.L. and Roberts, P.V., (1981). Transport of ion-exchanging solutes in groundwater: Chromatographic theory and field simulation, *Water Resources Research,* **17** (5), pp.1517-1527.
[37] Xie, Q., Saeedi, A., Pooryousefy, E. and Liu, Y., (2016). Extended DLVO-based estimates of surface force in low salinity water flooding, *Journal of Molecular Liquids,* **221** pp.658-665.
[38] Dzombak, D.A. and Morel, F.M., (1990). Surface Complexation Modeling: Hydrous Ferric Oxide. John Wiley & Sons.
[39] Kuznetsov, D., Cotterill, S., Giddins, M.A. and Blunt, M.J., (2015). Low-salinity waterflood simulation: Mechanistic and phenomenological models, *SPE Asia Pacific Enhanced Oil Recovery Conference,*
[40] Al-Shalabi, E.W. and Sepehrnoori, K., (2016). A comprehensive review of low salinity/engineered water injections and their applications in sandstone and carbonate rocks, *Journal of Petroleum Science and Engineering,* **139** pp.137-161.
[41] Omekeh, A.V., Evje, S. and Friis, H.A., (2012). Modeling of low salinity effects in sandstone oil rocks, *Int.J.Numer.Anal.Model,* **1** pp.1-18.
[42] Dang, C.T.Q., Nghiem, L.X., Chen, Z.J. and Nguyen, Q.P., (2013). Modeling low salinity waterflooding: Ion exchange, geochemistry and wettability alteration, *SPE Annual Technical Conference and Exhibition,*
[43] Kazemi Nia Korrani, A., Jerauld, G.R. and Sepehrnoori, K., (2016). Mechanistic modeling of low-salinity waterflooding through coupling a geochemical package with a compositional reservoir simulator, *SPE Reservoir Evaluation & Engineering,* **19** (01), pp.142-162.

[44] Korrani, A.K. and Jerauld, G.R., (2019). Modeling wettability change in sandstones and carbonates using a surface-complexation-based method, *Journal of Petroleum Science and Engineering,* **174** pp.1093-1112.
[45] Chapman, D.L., (1913). LI. A contribution to the theory of electrocapillarity, *The London, Edinburgh, and Dublin Philosophical Magazine and Journal of Science,* **25** (148), pp.475-481.
[46] Stern, O., (1924). *Zur Theorie Der Elektrolytischen Doppelschicht.Z Elektrochem Angew Phys Chem 30, 508–516,*
[47] Wang, H. and Pilon, L., (2011). Accurate simulations of electric double layer capacitance of ultramicroelectrodes, *The Journal of Physical Chemistry C,* **115** (33), pp.16711-16719.
[48] Vinogradov, J., Jaafar, M. and Jackson, M., (2010). Measurement of streaming potential coupling coefficient in sandstones saturated with natural and artificial brines at high salinity, *Journal of Geophysical Research: Solid Earth,* **115** (B12),
[49] Glover, P.W. and Jackson, M.D., (2010). Borehole electrokinetics, *The Leading Edge,* **29** (6), pp.724-728.
[50] Bargar, J., Brown Jr, G. and Parks, G., (1997). Surface complexation of Pb (II) at oxide-water interfaces: II. XAFS and bond-valence determination of mononuclear Pb (II) sorption products and surface functional groups on iron oxides, *Geochimica Et Cosmochimica Acta,* **61** (13), pp.2639-2652.
[51] Vieira, A.R., (2006). *Surface Complexation Modeling of Pb (II), Cd (II) and Se (IV) Onto Iron Hydroxides in Single and Bisolute Systems,*
[52] Brady, P.V., Krumhansl, J.L. and Mariner, P.E., (2012). Surface complexation modeling for improved oil recovery, *SPE Improved Oil Recovery Symposium,*
[53] Brady, P.V. and Krumhansl, J.L., (2013). Surface complexation modeling for waterflooding of sandstones, *SPE Journal,* **18** (02), pp.214-218.
[54] Langmuir, D., (1997). Aqueous environmental, *Geochemistry Prentice Hall: Upper Saddle River, NJ,*
[55] Stokes, S.N., (2009). Diffuse layer modeling on iron oxides: Single and multi-solute systems on ferrihydrite and granular ferric hydroxide,
[56] Erzuah, S., Fjelde, I. and Omekeh, A.V., (2017). Wettability estimation by surface complexation simulations, *SPE Europec Featured at 79th EAGE Conference and Exhibition,*
[57] Elakneswaran, Y., Shimokawara, M., Nawa, T. and Takahashi, S., (2017). Surface complexation and equilibrium modeling for low salinity waterflooding in sandstone reservoirs, *Abu Dhabi International Petroleum Exhibition & Conference,*
[58] Parkhurst, D.L. and Appelo, C., (2013). *Description of Input and Examples for PHREEQC Version 3: A Computer Program for Speciation, Batch-Reaction, One-Dimensional Transport, and Inverse Geochemical Calculations,*
[59] Bethke, C., (1996). Geochemical Reaction Modeling: Concepts and Applications. Oxford University Press on Demand.
[60] Parkhurst, D.L. and Wissmeier, L., (2015). PhreeqcRM: A reaction module for transport simulators based on the geochemical model PHREEQC, *Advances in Water Resources,* **83** pp.176-189.
[61] Thyne, I.G., (2007). PHREEQC Modeling Short Course,
[62] Van Hal, R., Eijkel, J.C. and Bergveld, P., (1996). A general model to describe the electrostatic potential at electrolyte oxide interfaces, *Advances in Colloid and Interface Science,* **69** (1-3), pp.31-62.
[63] Takamura, K. and Chow, R.S., (1985). The electric properties of the bitumen/water interface Part II. Application of the ionizable surface-group model, *Colloids and Surfaces,* **15** pp.35-48.
[64] Dubey, S. and Doe, P., (1993). Base number and wetting properties of crude oils, *SPE Reservoir Engineering,* **8** (03), pp.195-200.
[65] Ghosh, P., (2012). Electrostatic double layer force: Part II, *NPTEL Chemical Engineering, Tutorial.URL Http://Nptel.Ac.in/Courses/103103033/Module3/Lecture3.Pdf,*
[66] Sanaei, A., Tavassoli, S. and Sepehrnoori, K., (2019). Investigation of modified Water chemistry for improved oil recovery: Application of DLVO theory and surface complexation model, *Colloids and Surfaces A: Physicochemical and Engineering Aspects,* **574** pp.131-145.
[67] Buckley, J., Takamura, K. and Morrow, N., (1989). Influence of electrical surface charges on the wetting properties of crude oils, *SPE Reservoir Engineering,* **4** (03), pp.332-340.
[68] Nasralla, R.A. and Nasr-El-Din, H.A., (2014). Impact of cation type and concentration in injected brine on oil recovery in sandstone reservoirs, *Journal of Petroleum Science and Engineering,* **122** pp.384-395.
[69] Vinogradov, J., Jackson, M.D. and Chamerois, M., (2018). Zeta potential in sandpacks: Effect of temperature, electrolyte pH, ionic strength and divalent cations, *Colloids and Surfaces A: Physicochemical and Engineering Aspects,* **553** pp.259-271.
[70] Al-Saedi, H.N., Flori, R.E. and Brady, P.V., (2019). Effect of divalent cations in formation water on wettability alteration during low salinity water flooding in sandstone reservoirs: Oil recovery analyses, surface reactivity tests, contact angle, and spontaneous imbibition experiments, *Journal of Molecular Liquids,* **275** pp.163-172.

Figures

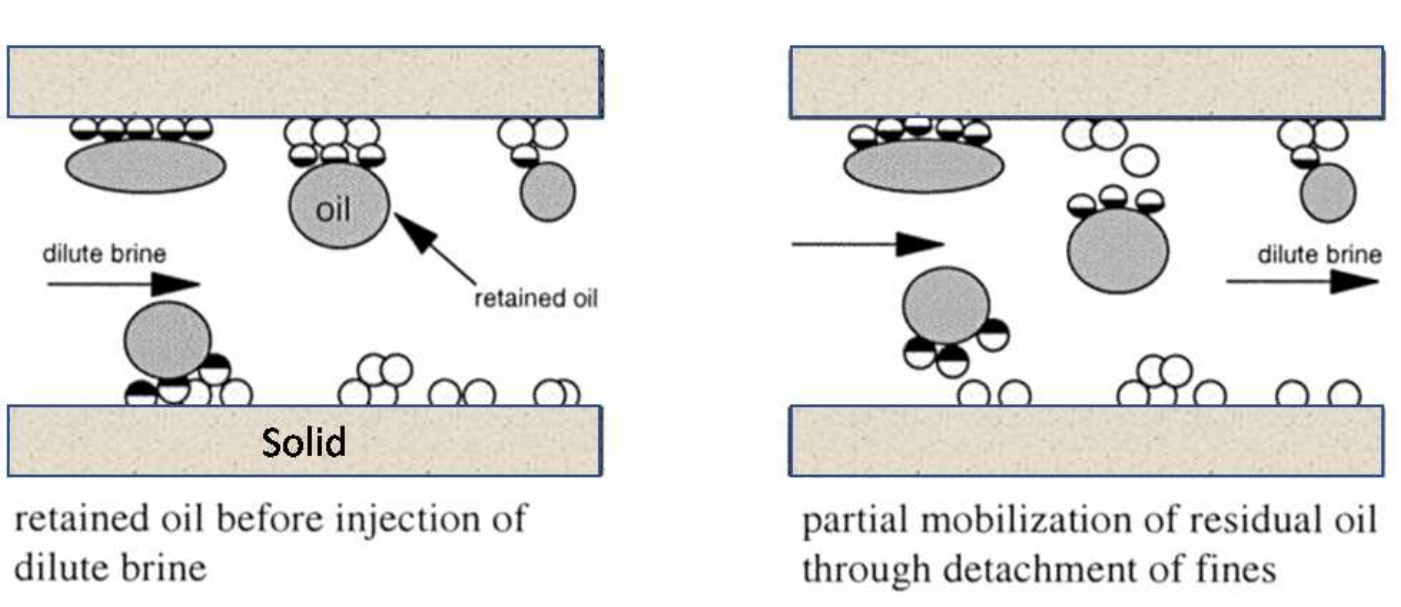

Figure 1

Fig. 1: Fine migration and clay-particles stripping mechanism [28].

Figure 2

Fig. 2: Proposed mechanism for oil desorption under the effect of LSWF flooding. Upper: the basic oil component desorption Lower: the acidic oil component desorption. [12].

Figure 3

Fig. 3: Oil adhesion mechanisms in the solid surface [16].

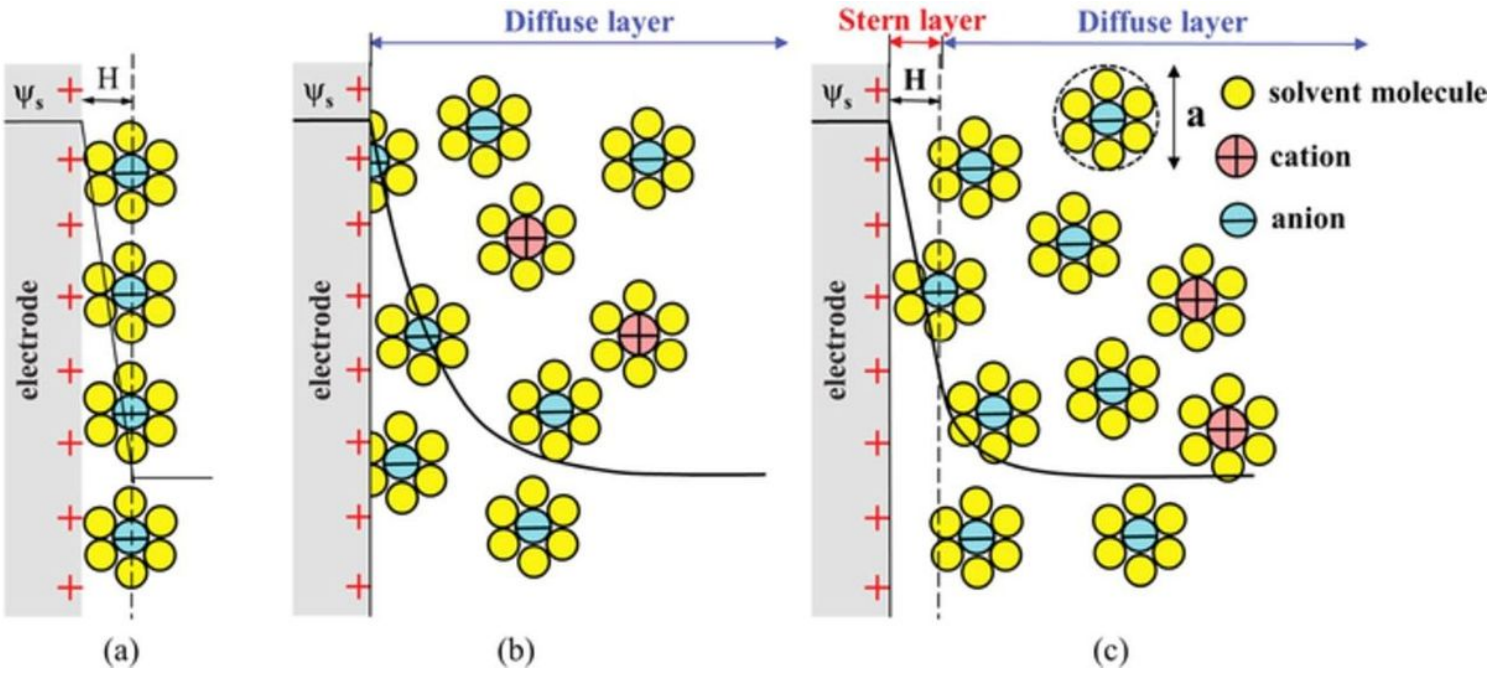

Figure 4

Fig. 4: Electrical double layer models with the distribution of the counter ions and co ions at the electrolyte/solution interface [47].

Figure 5

Fig. 5: Electrical double layer at the rock -brine interface [49].

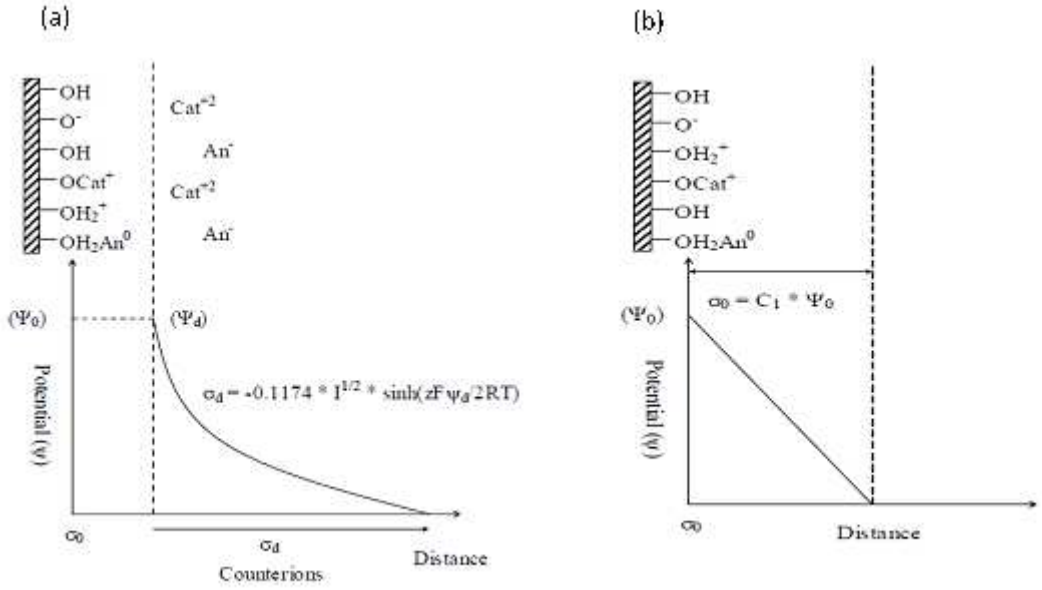

Figure 6

Fig. 6: Representation of the electric double layer (EDL) used in (a) the diffuse layer model [51].

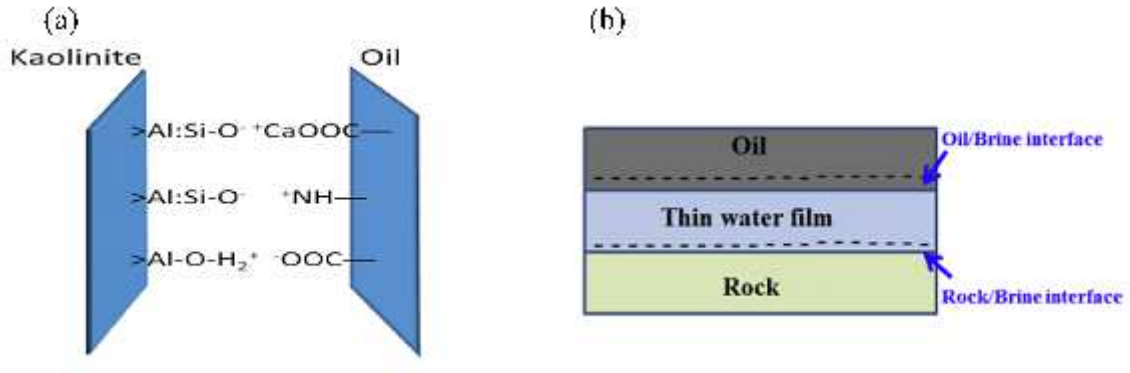

Figure 7

Fig. 7: a) Oil sandstone electrostatic pair linkages b) the thin water film between oil-brine and rock-brine interfaces [44, 52].

Figure 8

Fig. 8: Illustration of the steps used to predict the wettability alteration using SCMs.

Figure 9

Fig. 9: Measured zeta potential at the oil-brine interface compared with the PHREEQC output.

Figure 10

Fig. 10: Measured zeta potential at kaolinite-brine interface compared with the PHREEQC output.

Figure 11

Fig. 11: Charged surface groups configuration developed at (a) the kaolinite surface (b) the oil surface.

Figure 12

Fig. 12: Electrostatic pair linkages developed between the oil and kaolinite surfaces.

Figure 13

Fig. 13: The bond product sum prediction under the effect of different ionic strengths of injected brine.

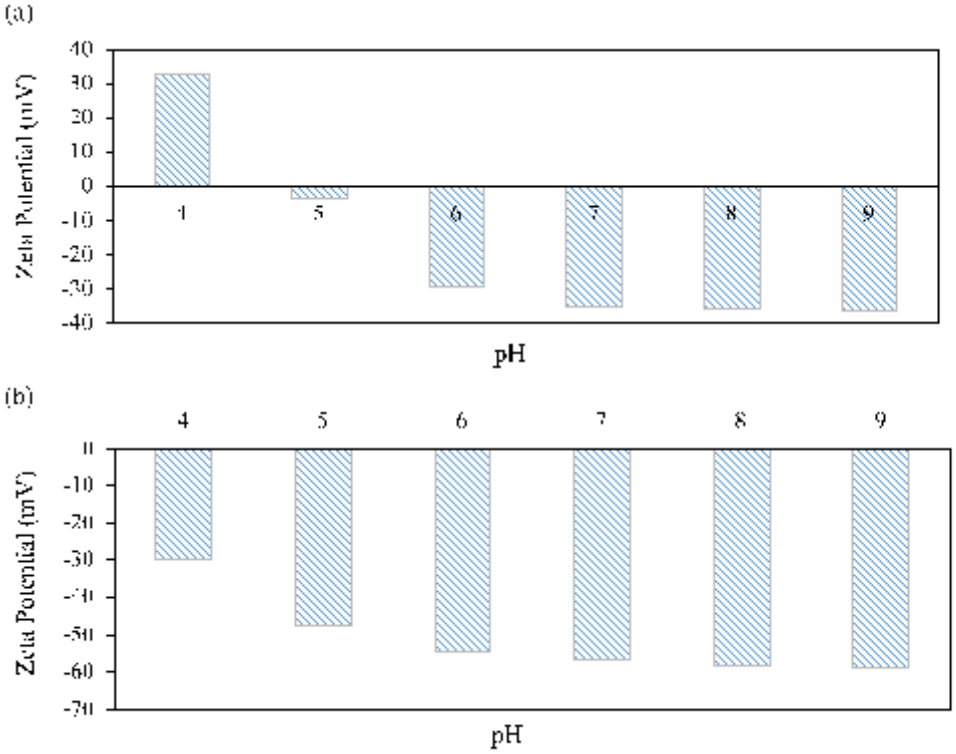

Figure 14

Fig. 14: Zeta potential development under the effect of pH, (a) oil surface (b) kaolinite surface.

Figure 15

Fig. 15: Zeta potential development under the effect of ionic strength at, (a) oil-brine interface (b) kaolinite-brine interface.

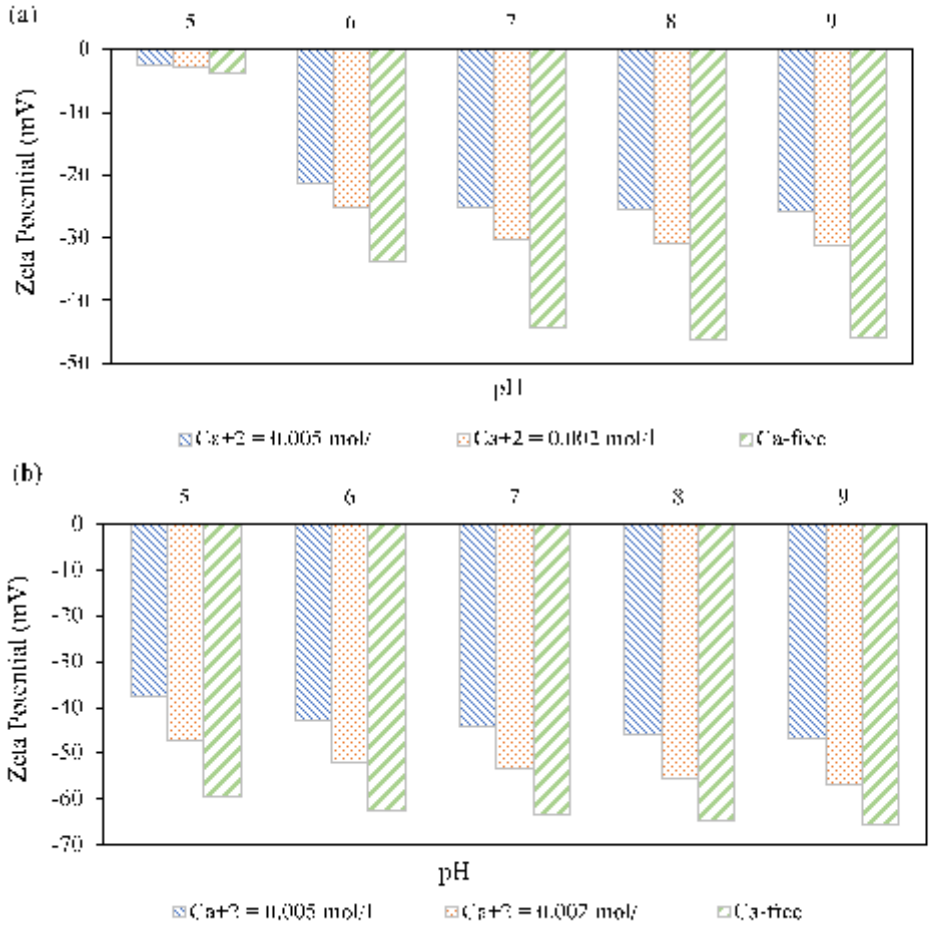

Figure 16

Fig. 16: Zeta potential development under the effect of divalent cation concentration in the injected brine, (a) oil-brine interface (b) kaolinite-brine interface.

Figure 17

Fig. 17: Stability number under the effect of the divalent cation concentration at pH 6.

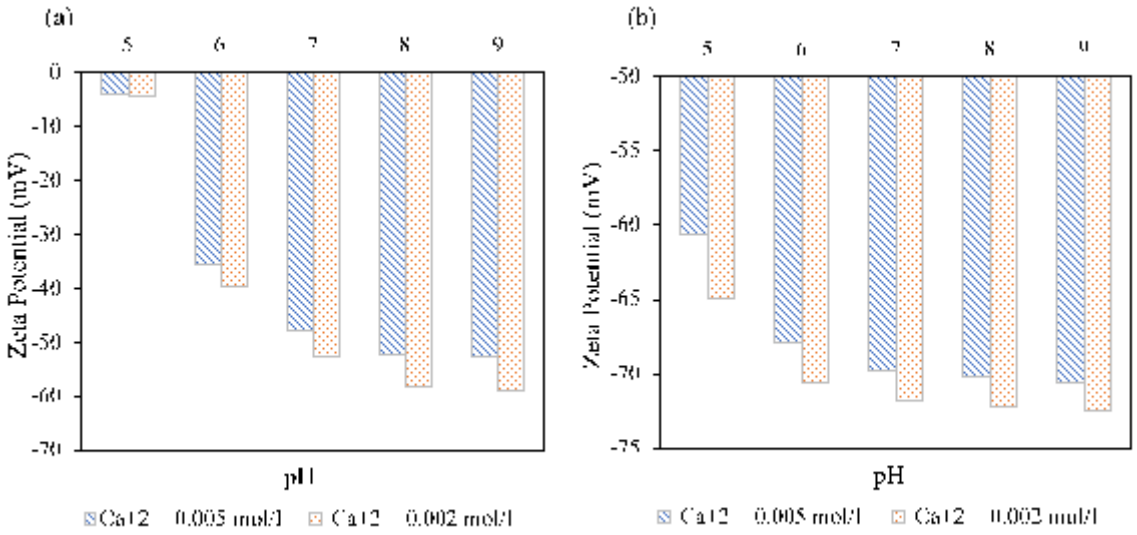

Figure 18

Fig. 18: Zeta potential development under the effect of divalent cation concentration in the formation water, (a) oil-brine interface (b) kaolinite-brine interface.

Figure 19

Fig. 19: stability number under the effect of divalent cation concentration in the formation water.

Figure 20

Fig. 20: Zeta potential development under the effect of divalent cation type, (a) oil-brine interface (b) kaolinite-brine interface.

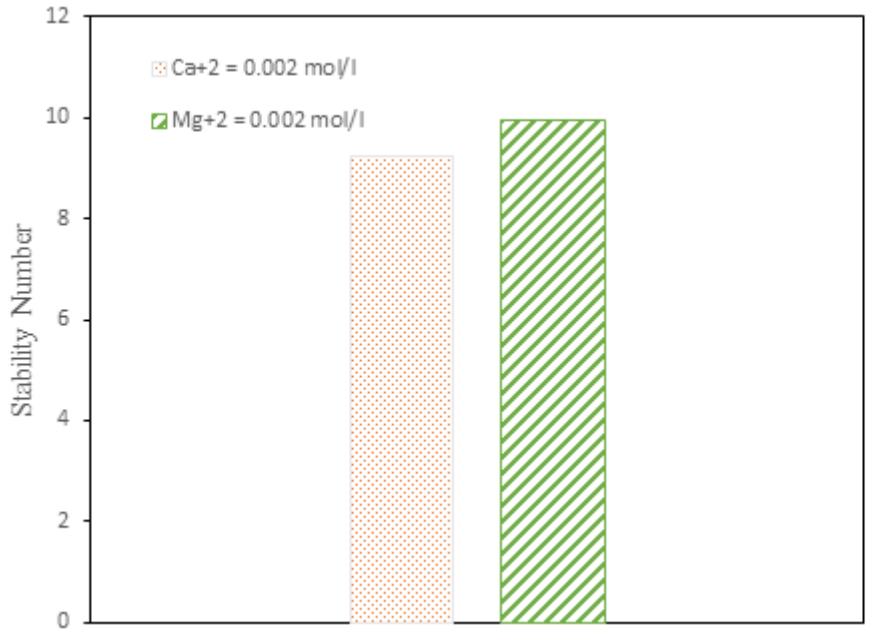

Figure 21

Fig. 21: stability number under the effect of divalent cation concentration in the formation water.

Figure 22

Fig. 22: Calcium carboxylate concentration at the oil surface under the effect of different Ca^{+2} level.

Figure 23

Fig. 23: Divalent cation sorbed affinity at the oil surface under the effect of divalent ions type.

Figure 24

Fig. 24: Zeta potential at different acid/base ratio, (a) oil-brine interface (b) kaolinite-brine interface.

Figure 25

Fig. 25: Stability number of crude oil emulsions with different acid/base ratios.